Inorganic Chemistry

Article

pubs.acs.org/IC

Molecular and Electronic Structures of Six-Coordinate "Low-Valent" $[M(^{Me}bpy)_3]^0$ (M = Ti, V, Cr, Mo) and $[M(tpy)_2]^0$ (M = Ti, V, Cr), and Seven-Coordinate $[MoF(^{Me}bpy)_3](PF_6)$ and $[MX(tpy)_2](PF_6)$ (M = Mo, X = Cl and M = W, X = F)

Mei Wang, Thomas Weyhermüller, Jason England, and Karl Wieghardt*

Max Planck Institute for Chemical Energy Conversion, Stiftstrasse 34-36, D-45470 Mülheim an der Ruhr, Germany

Supporting Information

ABSTRACT: The electronic structures of a series of so-called "low-valent" transition metal complexes $[M(^{Me}bpy)_3]^0$ and $[M(tpy)_2]^0$ (^{Me}bpy = 4,4′-dimethyl-2,2′-bipyridine and tpy = 2,2′,6′,2″-terpyridine) have been determined using a combination of X-ray crystallography, magnetochemistry, and UV–vis–NIR spectroscopy. More specifically, the crystal structures of the long-known complexes $[Ti^{IV}(tpy^{2-})_2]^0$ (S = 0, **6**), $[V^{IV}(tpy^{2-})_2]$ (S = $^1/_2$, **7**), $[Ti^{III}(^{Me}bpy^{\bullet})_3]^0$ (S = 0, **1**), $[V^{II}(^{Me}bpy^{\bullet})_2(^{Me}bpy^0)]^0$ (S = $^1/_2$, **2**), and $[Mo^{III}(^{Me}bpy^{\bullet})_3]^0$ (S = 0, **4**) have been determined for the first time. In all cases, the experimental results confirm the electronic structure assignments that we ourselves have recently proposed. Additionally, the six-coordinate complex $[Mo^{III}(bpy^0)_2Cl_2]Cl{\cdot}2.5CH_3OH$ (S = $^3/_2$, **13**), and seven-coordinate species $[Mo^{IV}F(^{Me}bpy^{\bullet})_2(^{Me}bpy^0)](PF_6)$ (S = 0, **5**), $[Mo^{IV}Cl(tpy^{\bullet})_2](PF_6){\cdot}CH_2Cl_2$ (S = 0, **11**), and $[W^{V}F(tpy^{\bullet})(tpy^{2-})](PF_6){\cdot}CH_2Cl_2$ (S = 0, **12**) have been synthesized and, for the first time, crystallographically characterized. Using the resulting data, plus that from previously published high-resolution X-ray structures of analogous compounds, it is shown that there is a linear correlation between the average $C_{py}{-}C'_{py}$ bond distances in these complexes and the total charge (n) of the ligands, $\{(bpy)_3\}^n$ and $\{(tpy)_2\}^n$. Hence, an assignment of the total charge of coordinated bpy or tpy ligands and, by extension, the oxidation state of the central metal ion can reliably be made on the basis of X-ray crystallography alone. In this study, the oxidation states of the metal ions range from +II to +V and in no case has an oxidation state of zero been validated. It is, therefore, highly misleading to use the term "low-valent" to describe any of the aforementioned neutral complexes.

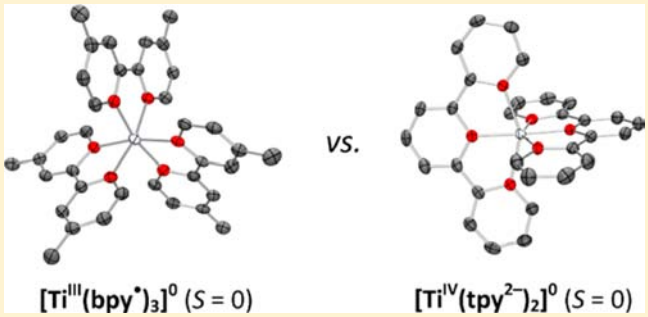

INTRODUCTION

Many homoleptic, neutral, six-coordinate $[M(bpy)_3]^0$ and $[M(tpy)_2]^0$ (bpy = 2,2′-bipyridine and tpy = 2,2′,6′,2″-terpyridine) complexes of transition metal ions have been synthesized in the past sixty years, and are listed in Tables 1 and 2, respectively.[1] These compounds have often been referred to as "low-valent" species composed of a formally zerovalent metal ion and neutral (bpy^0) and (tpy^0) ligands. In an effort to elucidate their true electronic structures, a number of intense spectroscopic investigations have been reported,[1] often with controversial and contradictory results. For example, for $[Cr(bpy)_3]^0$ and $[Cr(tpy)_2]^0$ it became clear in ∼1970 that the central chromium ion does not possess a low spin d^6 electron configuration. Instead, the participation of empty π^* ligand-based lowest unoccupied molecular orbitals (LUMOs) in the binding was invoked, mostly in terms of "π-back donation" effects, but also via reduction of one or all ligands.[1] Thus, definitive assignment of the ligand redox states(s) and, concomitantly, oxidation state (its d^n electron configuration) of the central metal ion remained elusive.

Recently, it has been unequivocally established by us,[2−6] and Goicoechea, McGrady and co-workers[7,8] that both bpy and tpy can coordinate to a given metal ion as either a neutral ligand, (bpy^0) and (tpy^0),[9] paramagnetic π-radical anions, $(bpy^{\bullet})^-$ and $(tpy^{\bullet})^-$, or diamagnetic dianions, $(bpy^{2-})^{2-}$ and $(tpy^{2-})^{2-}$. These conclusions are largely based upon high resolution X-ray crystallography at cryogenic temperatures (∼100 K), but are also corroborated by density functional theoretical calculations and comprehensive spectroscopic studies (e.g., X-ray absorption spectroscopy, XAS, and electron paramagnetic resonance, EPR).

In the case of bpy, its three ligand oxidation levels $(bpy)^n$ (n = 0, 1−, 2−) differ significantly in terms of structural parameters and can therefore be readily discerned by X-ray crystallography.[2−11] More specifically, population of the π^* LUMO of (bpy^0) upon one and two electron reduction affects a shortening of the interpyridine $C_{py}{-}C_{py}$ bond and a lengthening of the neighboring C–N bonds (see Figure 5).[9] It should

Received: August 7, 2013
Published: October 11, 2013

   dx.doi.org/10.1021/ic402037e | *Inorg. Chem.* 2013, 52, 12763−12776

Table 1. Previously Reported Neutral *tris*(bpy) Metal Complexes That Have Been Isolated as Solids

complex	ground state (S)	synthesis ref.[a]
$[Al^{III}(bpy^{\bullet})_3]^0$	$^1/_2$	13a
$[Mg^{II}(bpy^{\bullet})_2(bpy^0)]^0$	0	13b
$[Sc^{III}(bpy^{\bullet})_3]^0$	$^1/_2$	13c
$[Y^{III}(bpy^{\bullet})_3]^0$	$^1/_2$	13d
$[Ti^{III}(bpy^{\bullet})_3]^0$	0	13e
$[Zr^{IV}(bpy^{\bullet})_2(bpy^{2-})]^0$	0	13f
$[Hf^{IV}(bpy^{\bullet})_2(bpy^{2-})]^0$	0	13g
$[V^{II}(bpy^{\bullet})_2(bpy^0)]^0$	$^1/_2$	13h
$[Nb^{IV}(bpy^{2-})_2(bpy^0)^0$	$^1/_2$	13i
$[Ta^{V}(bpy^{\bullet})(bpy^{2-})_2]^0$	$^1/_2$	13j
$[Cr^{III}(bpy^{\bullet})_3]^0$	0	13k
$[Mo^{III}(bpy^{\bullet})_3]^0$	0	13l
$[Mn^{II}(bpy^{\bullet})_2(bpy^0)]^0$	$^3/_2$	13m
$[Re(bpy)_3]^0$		13n
$[Fe^{II}(bpy^{\bullet})_2(bpy^0)]^0$	1[b]	13o, p
$[Ru^{II}(bpy^{\bullet})_2(bpy^0)]^0$	0	13q
$[Os(bpy^{\bullet})_2(bpy^0)]^0$	0	13r
$[Co(bpy)_3]^0$		13s

[a]The references correspond to the first report of synthesis and isolation of the complex. [b]The ground state was DFT calculated only.[10]

Table 2. Previously Reported Neutral *bis*(tpy) Metal Complexes That Have Been Isolated as Solids

complex	ground state (S)	synthesis ref.[b]	X-ray structure ref.
$[Ti^{IV}(tpy^{2-})_2]^0$ (**6**)	0	14a	this work
$[V^{IV}(tpy^{2-})_2]^0$ (**7**)	$^1/_2$	14b, c	this work
$[Cr^{III}(tpy^{\bullet})(tpy^{\bullet\bullet})]^0$ (**8**)	0	14d	16
$[Mo^{IV}(tpy^{2-})_2]^0$ (**9**)	0	14e, f	16
$[W^{V}(tpy^{2-})(tpy^{3-})]^0$ (**10**)	0	14g	16
$[Fe^{II}(tpy^{\bullet})_2]^0$	1[a]	4	4
$[Ru^{II}(tpy^{\bullet})_2]^0$	1[a]	14h	14h
$[Os^{II}(tpy^{\bullet})_2]^0$	0	14i	

[a]Values taken from reference 4. [b]The references correspond to the first report of synthesis and isolation of the complex.

be highlighted that whereas both (bpy^0) and the radical anion $(bpy^{\bullet})^-$ are very weak π-acceptors, the dianion $(bpy^{2-})^{2-}$ is a strong π-donor.[10] Furthermore, π-back-donation from an electron rich metal to a (bpy^0) ligand does not, in general, lead to significant structural changes and cannot be detected by X-ray crystallography. This is quite simply because the energy difference between the π^* LUMO of the (bpy^0) ligand and the occupied metal-centered t_{2g} (in O_h symmetry) orbitals is too large for effective overlap. The same is also true of the $(bpy^{\bullet})^-$, which is a good σ-donor ligand but displays no significant π-acceptor capacity. In other words, $C_{py}-C_{py}$ and C–N bond distances in five-membered $M(bpy^0)$ and $M(bpy^{\bullet})$ chelates closely resemble those of uncoordinated (bpy^0) molecules and alkali metal salts of $(bpy^{\bullet})^-$ anions, respectively.[9] On the other hand, the N,N'-coordinated dianion $(bpy^{2-})^{2-}$ is a strong π-donor, and coordination to an electron-poor transition metal ion, such as that with a d^0 electron configuration, is accompanied by a significant lengthening of the $C_{py}-C_{py}$ bond up to a length of ~1.40 Å from 1.36 Å in alkali metal salts of the dianion.[9d]

These statements regarding bpy apply equally well to the tpy ligand. Not only is (tpy^0) a very weak π-acceptor, reduction of the N,N',N''-coordinated neutral ligands by one and two electrons also leads to a sequential decrease of the average $C_{py}-C_{py}$ distance from 1.48 ± 0.01 Å in (tpy^0), to 1.45 ± 0.01 Å in $(tpy^{\bullet})^-$, and 1.43 ± 0.01 Å in the singlet or triplet dianions, $(tpy^{2-})^{2-}$ and $(tpy^{\bullet\bullet})^{2-}$.[16] The triplet dianion $(tpy^{\bullet\bullet})^{2-}$ is an excited state that can be accessed because of close energetic proximity of the LUMO and LUMO+1 orbitals, which would in principle also allow access to a trianion $(tpy^{3-})^{3-}$ ($S = ^1/_2$) and tetraanion $(tpy^{4-})^{4-}$ ($S = 0$). Indeed, the radical anion $(tpy^{3-})^{3-}$ has been invoked as a ligand in $[W(tpy)_2]^0$ and calculated to possess an average $C_{py}-C_{py}$ distance of 1.402 Å.[16] Since the stepwise addition of one to three electrons to the neutral (tpy^0) ligand has a small impact upon the average $C_{py}-C_{py}$ distance (~0.03 Å with each redox event), determination of the oxidation state of the ligand in a given complex requires that the crystal structure is of very high quality. In fact, a very small estimated standard deviation σ of <0.004 Å is required, which means that the crystal must be devoid of disorder or twinning problems.

Although early attempts, published in 1963, were made to record an X-ray structure for *neutral* $[M(bpy)_3]^0$ (M = Ti, V, and Cr) complexes using film techniques (these efforts were severely hampered by twinning problems),[13t] the first crystallographically well characterized example $[Ru(bpy)_3]^0$ ($S = 0$) was not published until 1997.[12] We recently succeeded in obtaining a high quality structure of $[Cr(^{Me}bpy)_3]^0$ ($S = 0$),[11,15] which was only the second crystal structure of such a compound, and herein we report the corresponding Ti, V, and Mo structures (Chart 1).[15] In contrast to the scarcity of published $[M(bpy)_3]^0$ structures, several neutral $[M(tpy)_2]^0$ complexes have been crystallographically characterized, namely $[Ru^{II}(tpy^{\bullet})_2]^0$ ($S = 0$),[14h] $[Fe^{II}(tpy^{\bullet})_2]^0$ ($S = 1$),[4] $[Cr^{III}(tpy^{\bullet})(tpy^{\bullet\bullet})]^0$ ($S = 0$),[16] $[Mo^{IV}(tpy^{2-})_2]^0$ ($S = 0$),[16] and $[W^{V}(tpy^{2-})(tpy^{3-})]^0$ ($S = 0$).[16] In this manuscript, this series has been extended to include the analogous Ti and V complexes. Additionally, we have included the synthesis and crystallographic characterization of the formally divalent seven-coordinate complexes $[MoCl(tpy)_2]\cdot(PF_6)\cdot CH_2Cl_2$, $[WF(tpy)_2](PF_6)\cdot CH_2Cl_2$, and $[MoF(^{Me}bpy)_3]\cdot(PF_6)$, plus the 6-coordinate complex $[Mo^{III}(bpy^0)_2Cl_2]Cl$. The electronic structures of the aforementioned complexes have been interrogated using a combination of X-ray crystallography, magnetochemistry, and EPR and UV–vis–NIR spectroscopies. This data provided allowed construction of correlations between experimental structural parameters of $\{bpy_3\}^n$ and $\{tpy_2\}^n$ and their total charge (n), thereby providing a means to accurately assign the average redox states of these ligands in related complexes using only X-ray crystallographic data. This is illustrated for $[M(bpy)_2(OR)_2]^0$ (M = Mo,[9a,17] W,[18] and Ti;[19] $(OR)^-$ = isopropylate or 2,3,5,6-tetraphenylphenolate), complexes that were central to studies that promoted the erroneous notion that bpy ligands have significant π-accepting properties, and used to reinterpret their electronic structures.

EXPERIMENTAL SECTION

Synthesis of Compounds. Unless stated otherwise, all syntheses were carried out in the absence of water and dioxygen under an Ar blanketing atmosphere using standard Schlenk techniques or a glovebox. The starting material $[MoCl_3(THF)_3]^0$[20] and complexes **3**,[11] **8**,[16] **9**,[16] and **10**[16] were prepared according to literature procedures. All other reagents were purchased from Sigma-Aldrich and used without further purification.

dx.doi.org/10.1021/ic402037e | Inorg. Chem. 2013, 52, 12763–12776

Chart 1. Designations and Ground States of Complexes Discussed in This Study

Complex [a]	Designation	Ground State (*S*)	Ref.
$[Ti(^{Me}bpy)_3]^0$	**1**	0	this work
$[V(^{Me}bpy)_3]^0$	**2**	1/2	this work
$[Cr(^{Me}bpy)_3]^0$	**3**	0	11
$[Mo(^{Me}bpy)_3]^0$	**4**	0	this work
$[MoF(^{Me}bpy)_3](PF_6)$	**5**	0	this work
$[Ti(tpy)_2]^0$	**6**	0	this work
$[V(tpy)_2]^0$	**7**	1/2	this work
$[Cr(tpy)_2]^0$	**8**	0	16
$[Mo(tpy)_2]^0$	**9**	0	16
$[W(tpy)_2]^0$	**10**	0	16
$[MoCl(tpy)_2](PF_6)\cdot CH_2Cl_2$	**11**	0	this work
$[WF(tpy)_2](PF_6)\cdot CH_2Cl_2$	**12**	0	this work
$[Mo(bpy)_2Cl_2]Cl\cdot 2.5CH_3OH$	**13**	3/2	this work
$[Mo(bpy)_2(O^iPr)_2]^0$	**14**	0	9a, 17
$[W(bpy)_2(OAr)_2]^0$ [b]	**15**	0	18

[a] bpy = 2,2′-bipyridine; ^{Me}bpy = 4,4′-dimethyl-2,2′-bipyridine; tpy = 2,2′:6′,2″-terpyridine. [b] ArO^- = 2,3,5,6-tetraphenylphenolate.

*$[Ti(^{Me}bpy)_3]^0$ (**1**).* ^{Me}bpy (0.55g; 3.0 mmol) was added to a suspension of $TiCl_3$ (0.154 g; 1.0 mmol) and Na amalgam (5 wt %) in 25 mL of tetrahydrofuran (THF) and stirred at ambient temperature for 48 h. The resulting dark blue solution was filtered, and the filtrate reduced to dryness in vacuo. The residue obtained was dissolved in dry toluene and filtered. Removal of the solvent from the flitrate in vacuo afforded 0.32 g (35% yield) of the product $[Ti(^{Me}bpy)_3]$. X-ray quality dark blue crystals were grown at −20 °C by vapor diffusion of *n*-pentane into a saturated toluene solution of **1**. Anal. Calcd. for $C_{36}H_{36}N_6Ti$: C, 71.99; H, 6.04; N, 13.99. Found: C, 71.78; H, 6.17; N, 14.22.

*$[V(^{Me}bpy)_3]^0$ (**2**).* This complex was obtained in 61% yield (0.37 g) via an analogous procedure to that described for **1**, but using VCl_3 in place of $TiCl_3$. X-ray quality crystals were grown at −20 °C by vapor diffusion of diethylether into a saturated THF solution of **2**. Anal. Calcd. for $C_{36}H_{36}N_6V$: C, 71.63; H, 6.01; N, 13.92. Found: C, 71.40; H, 6.12; N, 13.74.

*$[Mo(^{Me}bpy)_3]^0$ (**4**).* This compound was prepared 57% yield (0.37 g) via an analogous procedure to that described for **1**, but using $[MoCl_3(THF)_3]^0$ in place of $TiCl_3$. X-ray quality black crystals were grown at −20 °C by vapor diffusion of *n*-pentane into a saturated THF solution of **4**. Anal. Calcd. for $C_{36}H_{36}N_6Mo$: C, 66.66; H, 5.59; N, 12.96. Found: C, 66.49; H, 5.79; N, 12.78.

*$[MoF(^{Me}bpy)_3](PF_6)$ (**5**).* At room temperature, a solution of ferrocenium hexafluorophosphate (0.33 g; 1.0 mmol) in THF (10 mL) was added dropwise to a black solution of **4** (0.65 g; 1.0 mmol) in THF (10 mL) and stirred for 18 h. The solvent of the resultant black-purple solution was removed in vacuo and, to remove ferrocene byproduct, the residual black solid was washed several times with Et_2O. The residue was then dried in vacuo, dissolved in CH_3CN (15 mL), filtered, and all volatiles removed from the filtrate to provide the product as a black-purple powder (yield: 0.29 g, 36%). X-ray quality crystals were grown by vapor diffusion of Et_2O into a saturated acetonitrile solution of **5**. Anal. Calcd. for $C_{36}H_{36}F_7N_6MoP$: C, 53.21; H, 4.47; N, 10.34. Found: C, 53.35; H, 4.72; N, 9.98.

*$[Ti(tpy)_2]^0$ (**6**).* This compound was prepared via two different procedures, one described in ref 14a and the other analogous to that described above for **1**. Both provided the same material, but the latter proceeded in higher yield. Anal. Calcd. for $C_{30}H_{22}N_6Ti$: C, 70,04; H, 4.31; N, 16.34. Found: C, 70.21; H, 4.1; N, 16.22.

*$[V(tpy)_2]^0$ (**7**).* This compound was prepared via two different procedures, one described in ref 14b and the other analogous to that described above for **1**. Both provided the same material, but the latter proceeded in higher yield. Anal. Calcd. for $C_{30}H_{22}N_6V$: C, 69.63; H, 4.28; N, 16.24. Found: C, 69.81; H, 4.31; N, 16.05.

*$[MoCl(tpy)_2](PF_6)\cdot CH_2Cl_2$ (**11**).* A dichloromethane (10 mL) solution of $[Mo(tpy)_2]^0$ (56 mg, 0.1 mmol) was added to a suspension of $AgPF_6$ (25 mg, 0.1 mmol) in CH_2Cl_2 (10 mL), and the resulting mixture stirred for 2 h at room temperature. Precipitated Ag was removed by filtration and the filtrate reduced to ∼1/3 of its original volume under vacuum, whereupon the formation of black microcrystals (yield: 28 mg, 31%.) suitable for X-ray crystallography was observed. Anal. Calcd. for $C_{31}H_{24}Cl_3F_6N_6PMo$: C, 44.94; H, 2.92; N, 10.15. Found: C, 44.73; H, 2.82; N, 10.32.

*$[WF(tpy)_2](PF_6)\cdot CH_2Cl_2$ (**12**).* This compound was prepared in 31% yield (28 mg) via an analogous procedure to that described for **11**, but using $[W(tpy)_2]^0$ in place of $[Mo(tpy)_2]^0$. Anal. Calcd. for $C_{31}H_{24}Cl_2F_7N_6PW$: C, 41.40; H, 2.69; N, 9.34. Found: C, 41.23; H, 2.41; N, 9.15.

*$[Mo(bpy)_2Cl_2]Cl\cdot 2.5CH_3OH$ (**13**).* Addition of bpy (0.47 g; 3.0 mmol) to a methanol (20 mL) solution of $[MoCl_3(THF)_3]$ (0.42 g, 1.0 mmol) afforded a dark red solution, which was stirred for 24 h at room temperature. The microcrystalline dark red solid formed during this time was collected by filtration, washed with Et_2O and dried in vacuo to give the product in 67% yield (0.40 g). X-ray quality crystals of **13** were grown by vapor diffusion of Et_2O into a saturated CH_3OH

dx.doi.org/10.1021/ic402037e | *Inorg. Chem.* 2013, 52, 12763−12776

Table 3. Crystallographic Data for Complexes 1, 2, 4−7, and 11−13

	1	2	4	5	6	7	11·CH_2Cl_2	12·CH_2Cl_2	13
chem. formula	$C_{36}H_{36}N_6Ti$	$C_{36}H_{36}N_6V$	$C_{36}H_{36}MoN_6$	$C_{36}H_{36}F_7MoN_6P$	$C_{30}H_{22}N_6Ti$	$C_{30}H_{22}N_6V$	$C_{31}H_{24}Cl_3F_6MoN_6P$	$C_{31}H_{24}Cl_2F_7N_6PW$	$C_{22.5}H_{26}Cl_3MoN_4O_{2.5}$
Fw	600.61	603.65	648.65	812.62	514.44	517.48	827.82	899.28	594.76
space group	$P2_1/n$, No. 14	$P2_1/n$, No. 14	$P2_1/c$, No. 14	*Pnma*, No. 62	*Fdd*2, No. 43	*Fdd*2, No. 43	$P2_1/c$, No. 14	$P2_1/c$, No. 14	$P\bar{1}$, No. 2
a, Å	11.763(2)	11.7239(13)	8.1571(15)	29.229(9)	39.123(5)	39.071(9)	9.548(2)	15.3478(13)	8.5901(9)
b, Å	18.532(4)	18.465(2)	20.239(4)	11.794(4)	56.678(7)	56.447(13)	19.208(3)	18.0554(9)	11.6333(13)
c, Å	14.613(3)	14.622(2)	18.567(4)	13.227(4)	8.4989(11)	8.390(2)	17.058(3)	11.7524(10)	14.163(2)
α, deg	90	90	90	90	90	90	90	90	109.056(3)
β, deg	109.727(3)	109.729(2)	97.038(3)	90	90	90	92.29(2)	109.264(7)	94.347(3)
γ, deg	90	90	90	90	90	90	90	90	109.704(2)
V, Å	2998.6(10)	2979.6(6)	3042.2(11)	4560(3)	18846(4)	18504(7)	3125.9(10)	3074.4(4)	1231.7(3)
Z	4	4	4	4	32	32	4	4	2
T, K	100(2)	100(2)	100(2)	100(2)	100(2)	100(2)	100(2)	100(2)	100(2)
ρ calcd, g cm^{-3}	1.330	1.346	1.416	1.184	1.451	1.486	1.759	1.943	1.604
refl. collected/$2\Theta_{max}$	36590/50.14	44299/56.94	61090/52.86	77233/50.00	135255/61.60	83085/49.42	95023/72.00	65675/66.16	730381/56.78
unique refl./$I > 2\sigma(I)$	5236/4399	7505/5961	6126/4737	4225/3823	14605/10515	7877/5725	14788/12843	11646/9054	6149/5022
no. of params/restr.	394/0	394/0	394/0	244/0	667/1	667/1	433/0	433/0	322/17
λ, Å /*μ*(K*α*), cm^{-1}	0.71073/3.22	0.71073/3.70	0.71073/4.67	0.71073/3.79	0.71073/3.97	0.71073/4.63	0.71073/7.99	0.71073/40.61	0.71073/8.88
R1[a]/goodness of fit[b]	0.0857/1.124	0.0661/1.149	0.0397/1.046	0.1017/1.166	0.0479/1.050	0.0466/1.015	0.0307/1.057	0.0391/1.099	0.0348/1.031
wR2[c] ($I > 2\sigma(I)$)	0.2419	0.1792	0.0787	0.2363	0.0905	0.0760	0.0748	0.0626	0.0816
residual density, e $Å^{-3}$	+1.31/−1.02	+1.07/−0.82	+0.53/−0.71	+2.94/−2.22	+0.48/−0.35	+0.25/−0.30	+1.16/−1.19	+2.96/−2.81	+1.33/−0.51

[a]Observation criterion: $I > 2\sigma(I)$. R1 = $\sum||F_o| - |F_c||/\sum|F_o|$. [b]GoF = $[\sum[w(F_o^2 - F_c^2)^2]/(n-p)]^{1/2}$. [c]wR2 = $[\sum[w(F_o^2 - F_c^2)^2]/\sum[w(F_o^2)^2]]^{1/2}$ where $w = 1/\sigma^2(F_o^2) + (aP)^2 + bP$, $P = (F_o^2 + 2F_c^2)/3$.

dx.doi.org/10.1021/ic402037e | Inorg. Chem. 2013, 52, 12763−12776

solution of complex. Anal. Calcd. for $C_{22.5}H_{26}O_{2.5}N_4Cl_3$: C, 45.40; H, 4.41; N, 9.42. Found: C, 45.19; H, 4.10; N, 9.65.

X-ray Crystallographic Data Collection and Refinement of the Structures. Single crystals of complexes **1**−**13** were coated with perfluoropolyether, picked up with nylon loops and mounted in the nitrogen cold stream of the diffractometer. Graphite monochromated Mo−Kα radiation (λ = 0.71073 Å) from a Mo-target rotating-anode X-ray source was used throughout. Final cell constants were obtained from least-squares fits of several thousand strong reflections. Intensity data were corrected for absorption using intensities of redundant reflections with the program SADABS.[21] The structures were readily solved by Patterson methods and subsequent difference Fourier techniques. The Siemens ShelXTL[22] software package was used for solution and rendering of the structures, ShelXL97[23] was used for the refinement. All non-hydrogen atoms were anisotropically refined, and hydrogen atoms were placed at calculated positions and refined as riding atoms with isotropic displacement parameters. Crystallographic data of the compounds are listed in Table 3.

RESULTS

The neutral *tris*(bpy) complexes **1**, **2**, and **4** were synthesized in THF solution under strictly anaerobic conditions by reaction of $TiCl_3$, VCl_3, and $MoCl_3$, respectively, with 3 equiv each of ^{Me}bpy and sodium amalgam (eq 1). Single crystals of these complexes suitable for X-ray crystallography were grown at −20 °C by vapor diffusion of *n*-pentane into concentrated toluene solutions of complex. (Synthesis and crystal structure of the corresponding Cr complex **3** is described in ref 11).

$$MCl_3(THF)_3 + 3(^{Me}bpy^0) + 3Na \xrightarrow{THF} [M(^{Me}bpy)_3]^0 + 3NaCl \quad M = Ti, V, Mo \qquad (1)$$

The neutral *bis*(tpy) complexes of Ti and V, **6** and **7**, were synthesized in analogous fashion by reaction of the appropriate metal trichloride with 2 equiv of the neutral ligand (tpy^0) and 3 equiv of sodium amalgam (eq 2). Single crystals of **6** and **7** suitable for X-ray analysis were obtained as described for the bpy complexes (Figure 2). The syntheses and crystal structures of **8**,[16] **9**,[15] **10**,[16] **14**,[9a,17] and **15**[18] have all been described in the literature.

$$MCl_3(THF)_3 + 2(typ^0) + 3Na \xrightarrow{THF} [M(tpy)_3]^0 + 3NaCl \quad M = Ti, V \qquad (2)$$

Attempts to generate the monocation $[Mo(^{Me}bpy)_3]^+$ by reaction of neutral **4** with 1 equiv of the one-electron oxidant ferrocenium hexafluorophosphate, $[Cp_2Fe](PF_6)$, yielded a purple-black solution from which single crystals of $[MoF(^{Me}bpy)_3](PF_6)$ (**5**) were grown. This was shown by X-ray crystallography (see below) to be a seven-coordinate monocationic species containing a fluoride ligand, which presumably derives from PF_6^-. Similarly, reaction of **9** with 1 equiv of the one-electron oxidant $Ag(PF_6)$ in CH_2Cl_2 solution afforded dark blue-crystals of diamagnetic $[MoCl(tpy)_2](PF_6)\cdot CH_2Cl_2$ (**11**), whose chloride ligand is most probably obtained from solvent. When the tungsten analogue of **9**, complex **10**, was used as a starting material under otherwise identical conditions, crystals of diamagnetic $[WF(tpy)_2](PF_6)\cdot CH_2Cl_2$ (**12**) were obtained in 31% yield.

Magnetic susceptibility data of solid samples of **1**, **3**,[11] **4**, **5**, **6**, **8**,[16] **9**,[16] **10**,[16] **11**, and **12** (Supporting Information, Figure S1) revealed that these complexes are all effectively diamagnetic over the temperature range 0−300 K, so possess an S = 0 ground state. In contrast, the vanadium species **2** and **7** both exhibit temperature-independent magnetic moments of ∼1.7(1) μ_B, indicative of $S = {}^1/_2$ ground states, and **13** possesses the quartet ground state ($S = {}^3/_2$) expected for a mononuclear octahedral Mo^{III} complex.

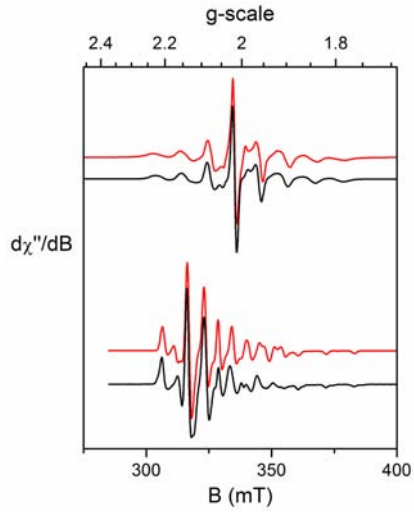

Figure 1. Top: X-band EPR spectrum of $[V(^{Me}bpy)_3]^0$ recorded in THF solution at 30 K (experimental conditions: frequency 9.4712 GHz; power 0.2 mW; modulation 10 G). Bottom: X-band EPR spectrum of $[V(tpy)_2]^0$ recorded in THF solution at 30 K (experimental conditions: frequency 9.47 GHz; power 0.2 mW; modulation 4 G). Experimental spectra and simulations are depicted using black and red lines, respectively.

EPR spectroscopy was used to probe the electronic structures of the vanadium complexes **2** and **7**, which are D_3 and D_{2d} symmetric, respectively. The X-band spectrum of **2** in frozen toluene solution at 30 K (Figure 1) is, unsurprisingly, very similar to those previously reported for $[V(bpy)_3]^0$ and $[V(^tbpy)_3]^0$ (see parameters in Table 4).[3] Its spectrum, which was simulated with g_{iso} = 1.984 and $|A_{iso}| = 78 \times 10^{-4}$ cm^{-1}, has an appearance consistent with a metal-based spin in a trigonal field. There is negligible anisotropy in the g-values with $g_x \sim g_y < 2.0$ and $g_z \approx 2.0$, but a large anisotropy in the axially split magnetic hyperfine interaction with $|A_{xx}| \sim |A_{yy}| > |A_{zz}|$, features characteristic of a metal-based singly occupied molecular orbital (SOMO) with a symmetry that in essence describes the vanadium d_{z^2} orbital.[3] Consistent with this picture, in a previously published density functional theory (DFT) study the a_1 SOMO was calculated to contain ∼90% V character, and it was concluded that the electronic structure of $[V(bpy)_3]^0$ is best described as $[V^{II}(bpy^\bullet)_2(bpy^0)]^0$, wherein $S = {}^1/_2$ ground state is obtained by antiferromagnetic coupling of the three unpaired electrons of the V^{II} ion with two $(bpy^\bullet)^-$ π-radical anions.[3]

The spectrum of **7** (Figure 1, bottom) is broadly similar to that of **2** with g_{iso} = 2.006 and $|A_{iso}| = 68 \times 10^{-4}$ cm^{-1}. However, it displays a small g anisotropy with $g_x \sim g_y \approx 2.0$ and $g_z < 2.0$, and a reversal of the $|A|$ anisotropy with $|A_{xx}| \sim |A_{yy}| < |A_{zz}|$. These parameters are typical of octahedral vanadium(IV) complexes, in which an unpaired electron resides in the d_{xy} orbital. Hence, the electronic structure of **7** is best described as $[V^{IV}(tpy^{2-})_2]^0$ containing two diamagnetic dianionic $(tpy^{2-})^{2-}$ ligands and a central $(d_{xy})^1$ V^{IV} ion.

Crystal Structures. We have determined the crystal structures of complexes **1**, **2**, **4**, **5**, **6**, **7**, **11**, **12**, and **13** at 100 K by high resolution X-ray crystallography (crystallographic

dx.doi.org/10.1021/ic402037e | Inorg. Chem. 2013, 52, 12763−12776

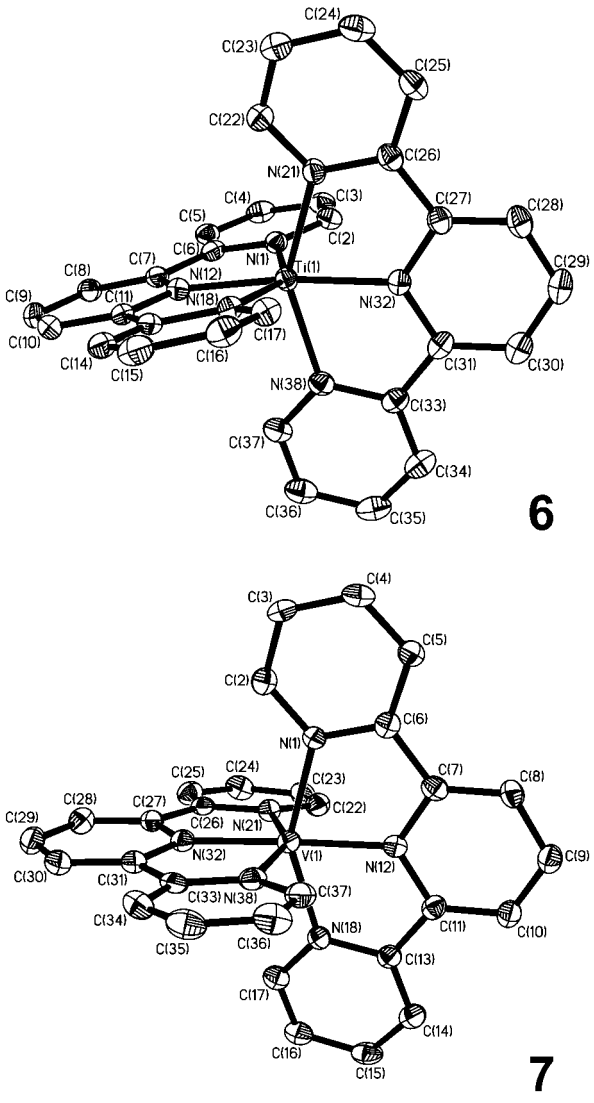

Figure 2. Structures of the neutral complexes **6** (top) and 7 (bottom) depicted using 40% probability ellipsoids. Hydrogen atoms have been omitted for clarity, and only one of two crystallographically independent molecules is shown.

details are summarized in Table 3). Selected bond distances for the bpy and tpy complexes are listed in Tables 5 and 6, respectively.

The structures of the neutral complexes $[M(tpy)_2]^0$ (M = Ti, V, Cr,[16] Mo,[16] W,[16] Fe,[4] Ru[14h]) all crystallize in the same orthorhombic space group *Fdd*2 with $Z = 32$ (2 crystallographically independent molecules per unit cell). In all cases, within the 3σ limits, the two crystallographically independent molecules per unit cell possess the same structural parameters, so are equivalent. Consequently, only one member of each pair is discussed subsequently. Regardless of the identity of the metal ion, the M−N bond to the central pyridine ring of the tpy ligand is always significantly shorter than those to the two terminal pyridine rings. The two short M−N bonds are *trans* oriented relative to one another, which gives rise to a compressed MN_6 octahedron of D_{2d} symmetry.

Previously, using K-edge X-ray absorption spectroscopy and X-ray crystallography we demonstrated that each member of the electron transfer series $[Cr(tpy)_2]^{3+,2+,1+,0}$ contains a central Cr^{III} ion with a t_{2g}^3 electron configuration.[16] Thus, the successive one-electron reductions that comprise the electron transfer series $[Cr^{III}(tpy^0)_2]^{3+} \rightarrow [Cr^{III}(tpy^{\bullet})(tpy^0)]^{2+} \rightarrow [Cr^{III}(tpy^{\bullet})_2]^{+} \rightarrow [Cr^{III}(tpy^{\bullet})(tpy^{\bullet\bullet})]^0$ involve occupation of π^* orbitals centered on the tpy ligands. Since these π^* ligand orbitals are bonding with respect to the $C_{py}-C_{py}$ bonds, the average distance between the pyridine rings in the tpy ligands $\{(tpy)_2\}^n$ decreases in a linear fashion with increasing charge (n), as shown in Figure 3. This holds true for other transition metals, and the resulting empirical correlation between the average $C_{py}-C_{py}$ bond distance and n in octahedral $[M(tpy)_2]^m$ complexes provides a means to determine n in other complexes using only their crystal structures.

For example, for complex **6** it can be deduced that $n = 4-$ (Figure 3), thereby rendering the oxidation state of the central titanium ion +IV and its electronic structure $[Ti^{IV}(tpy^{2-})_2]^0$ ($S = 0$). For the neutral vanadium complex **7** the observed average $C_{py}-C_{py}$ distance is also indicative that $n = 4-$, which means that its electronic structure is $[V^{IV}(tpy^{2-})_2]^0$ ($S = {}^1/_2$). In this formulation a single unpaired electron resides in a metal centered d_{xy}-orbital (compressed $V^{IV}N_6$ octahedron), which is consistent with its EPR spectrum. For complex **8** an electronic structure $[Cr^{III}(tpy^{\bullet})(tpy^{\bullet\bullet})]^0$ ($S = 0$) has been established,[16] in which the dianionic tpy ligand is coordinated in its triplet excited state. Together with the radical monanion, this provides three ligand-based unpaired spins that strongly couple antiferromagnetically with three unpaired electrons at the Cr^{III} ion and yield the observed $S = 0$ ground state of the complex. Previous studies suggest, and the correlation in Figure 3 concurs, that the electronic structure of the diamagnetic molybdenum complex **9** should be described as $[Mo^{IV}(tpy^{2-})_2]^0$.[16] In this scenario the singlet ground state could be attained by antiferromagnetic coupling of an excited triplet dianion $(tpy^{\bullet\bullet})^{2-}$ with the $S = 1$ Mo^{IV} ion. The second ligand dianion would then retain a singlet state, and the electronic structure of **9** would be $[Mo^{IV}(tpy^{\bullet\bullet})(tpy^{2-})]^0$. An analogous electronic structure has been proposed for the monoanion $[Cr^{III}(tpy^{\bullet\bullet})(tpy^{2-})]^-$ ($S = {}^1/_2$).[16] Alternatively, it is conceivable that in a compressed octahedral MoN_6 environment the central Mo^{IV} ion would be diamagnetic. Then to attain the $S = 0$ ground state observed for **9**, both ligands would also have to be diamagnetic $(tpy^{2-})^{2-}$ dianions.

Table 4. Spin Hamiltonian *g*- and *A*-Values Derived from Spectral Simulations of the X-band EPR Spectra of Complexes in Frozen Toluene Solution (30 K)

complex	g_{iso} [a]	g_x	g_y	g_z	A_{iso} [b]	A_{xx}	A_{yy}	A_{zz}
$[V^{II}(bpy^{\bullet})_2(bpy^0)]^{0c}$	1.983	1.981	1.981	1.988	−73.3	−86.0	−86.0	−48.0
$[V^{II}(^tbpy^{\bullet})_2(^tbpy^0)]^{0c}$	1.985	1.981	1.982	1.993	−77.9	−96.3	−96.3	−44.0
$[V^{II}(^{Me}bpy^{\bullet})_2(^{Me}bpy)]^0$ (**2**)	1.992	1.986	1.985	2.006	−76.8	−88.5	−102.1	−39.7
$[V^{IV}(tpy^{2-})_2]^0$ (**7**)	2.006	2.0304	2.0278	1.9612	−68.9	−48.8	−58.0	−100

[a] $g_{iso} = 1/3\ (g_x + g_y + g_z)$. [b] $A_{iso} = 1/3\ (A_{xx} + A_{yy} + A_{zz})$. [c] Values taken from reference 3.

Table 5. Intrachelate Bond Distances (Å) in ^{Me}bpy-Containing Transition Metal Complexes 1−5 and 13−14[a]

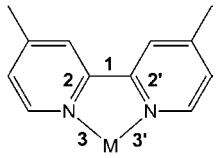

		^{Me}bpy(1)			^{Me}bpy(2)			^{Me}bpy(3)			
complex	M	1	2/2′	3/3′	1	2/2′	3/3′	1	2/2′	3/3′	ref.
1	Ti	1.431(6)	1.385(6)	2.099(4)	1.437(6)	1.390(6)	2.109(4)	1.428(6)	1.390(6)	2.100(4)	this work
2	V	1.436(4)	1.384(4)	2.071(2)	1.440(4)	1.383(4)	2.070(2)	1.439(4)	1.384(4)	2.074(2)	this work
3[b]	Cr	1.426(2)	1.384(1)	2.018(1)							11
4	Mo	1.427(4)	1.392(4)	2.104(3)	1.424(4)	1.381(5)	2.115(3)	1.428(4)	1.387(4)	2.117(3)	this work
5	Mo	1.439(10)	1.383(10)	2.188(6)	1.457(17)	1.382(9)	2.135(6)	1.439(10)	1.383(10)	2.188(6)	this work
13	Mo	1.474(3)	1.355(3)	2.163(2)	1.469(4)	1.357(3)	2.165(2)				this work
14	Mo	1.424(4)	1.370(4)	2.120(2)	1.425(4)	1.385(4)	2.115(2)				9a, 17
15	W	1.412(4)	1.383(3)	2.092(2)	1.409(4)	1.380(3)	2.106(2)				18

[a]Average values are given for bonds 2 and 2′, and for bonds 3 and 3′. A bond labeling scheme is provided above. [b]All three M(bpy) chelates are equivalent (i.e., crystallographic C_3 symmetry).

Table 6. Selected Bond Distances (Å) in $[M(tpy)_2]^0$-Containing Transition Metal Complexes 6−12[a]

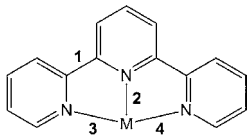

		tpy(1)				tpy(2)				
complex	M	1[b]	2	3	4	1[b]	2	3	4	ref.
6[c]	Ti	1.428(4)	2.026(2)	2.135(2)	2.123(2)	1.424(4)	2.021(2)	2.132(2)	2.142(2)	this work
7[c]	V	1.428(6)	1.970(3)	2.084(3)	2.090(3)	1.426(6)	1.967(3)	2.075(4)	2.081(4)	this work
8[c]	Cr	1.439(1)	1.940(1)	2.015(1)	2.012(1)	1.439(1)	1.938(1)	2.007(1)	2.019(1)	16
9[c]	Mo	1.433(4)	2.032(2)	2.096(2)	2.102(2)	1.434(4)	2.037(2)	2.100(2)	2.106(2)	16
10	W	1.418(5)	2.029(2)	2.083(2)	2.073(2)	1.425(5)	2.062(2)	2.072(2)	2.080(2)	16
11	Mo	1.446(2)	2.096(1)	2.124(1)	2.195(1)	1.449(2)	2.086(1)	2.132(1)	2.204(1)	this work
12	W	1.441(4)	2.066(3)	2.113(3)	2.171(3)	1.439(5)	2.070(3)	2.103(3)	2.176(3)	this work
	Fe	1.456(4)	2.043(2)	2.126(2)	2.144(2)	1.447(4)	2.041(2)	2.139(2)	2.150(2)	4
	Ru[d]	1.42(2)	1.98(1)	2.06(1)	2.05(1)	1.42(2)	1.99(1)	2.07(1)	2.08(1)	14h

[a]A bond labeling scheme is provided above. [b]Average of the 2 C_{py}−C_{py} bonds per ligand. [c]There are two crystallographically independent molecules per unit cell, whose bond lengths are identical within the 3σ limits. Hence, values are given for one molecule only. [d]Low quality structure with esd of approximately ±0.02 Å.

The neutral tungsten complex **10** displays the shortest average C_{py}−C_{py} distance (1.422 Å) in the entire $[M(tpy)_2]^0$ series. Using the empirical correlation in Figure 3, it can be concluded that the total ligand charge is $\{(tpy)_2\}^{5-}$, from which the electronic structure $[W^V(tpy^{2-})(tpy^{3-})]^0$ (S = 0) can be inferred. In this case, the experimentally observed diamagnetic ground state would derive from antiferromagnetic coupling of the unpaired electron of the d^1 W^V ion with the paramagnetic trianion $(tpy^{\bullet})^{3-}$ (S = $^1/_2$), leaving the dianion coordinated in its singlet ground state.[16]

As previously mentioned, complexes **11** and **12** contain the diamagnetic seven-coordinate monocations $[MoCl(tpy)_2]^+$ and $[WF(tpy)_2]^+$, respectively (Figure 4 and Table 6). The coordination polyhedra of both complexes can be described as distorted pentagonal bipyramidal, in which the central pyridine nitrogens of the two tpy ligands occupy the axial positions. Based upon the average C_{py}−C_{py} bond length in **11** of 1.448 Å, a sum ligand oxidation level of $\{(tpy)_2\}^{2-}$ can be deduced for **11**. Thus, its electronic structure is $[Mo^{IV}(tpy^{\bullet})_2Cl]^+$ and its diamagnetic ground state is obtained by antiferromagnetic coupling of the two $(tpy^{\bullet})^-$ radical ions with the central S = 1 Mo^{IV} ion. In contrast, the average C_{py}−C_{py} bond length in **12** of 1.440 Å suggests that a total ligand charge of $\{(tpy)_2\}^{3-}$ is appropriate, which would lead to the formulation $[W^VF(tpy^{\bullet})(tpy^{2-})]^+$, with its S = 0 ground state stemming from antiferromagnetic coupling of the single unpaired spin on the W^V ion with that of the $(tpy^{\bullet})^-$ radical monoanion (the dianion coordinates in its singlet ground state). However, as previously mentioned, the bond length changes observed upon oxidation/reduction of tpy are relatively small and high-resolution crystal structures with estimated standard deviations σ of <0.004 Å are required for accurate assignment of ligand oxidation state. Consequently, the resolution of the X-ray structure of **12** is insufficient for accurate assignment of its electronic structure, and alternative formulations as $[W^{VI}F(tpy^{2-})_2]^+$ and $[W^{IV}F(tpy^{\bullet})_2]^+$ cannot be ruled out.

Variation of the C_{py}−C_{py} and average C−N bond distances in $(bpy)^{n-}$, taken from X-ray structures of uncoordinated (bpy^0) and alkali metal salts of $(bpy^{\bullet})^-$ and $(bpy^{2-})^{2-}$,[9a,b,d] as a

dx.doi.org/10.1021/ic402037e | Inorg. Chem. 2013, 52, 12763−12776

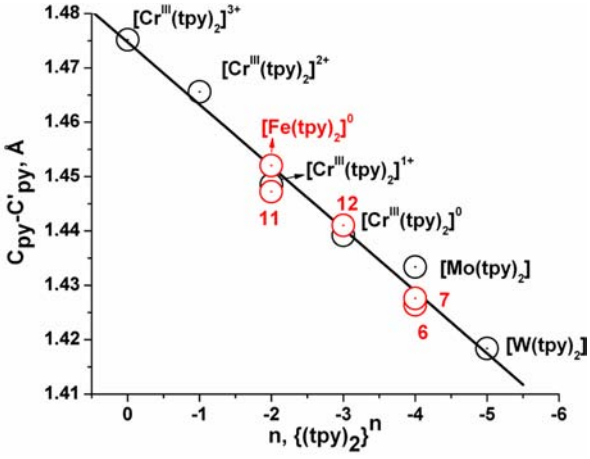

Figure 3. Average experimental $C_{py}-C'_{py}$ bond distances (Å) in $[M(tpy)_2]^m$ complexes as a function of total ligand $\{(tpy)_2\}^n$ charge (n). Data for $[Cr(tpy)_2]^m$ (m = 3+, 2+, 1+, 0) and $[M(tpy)_2]^0$ (M = Mo, W; black points) taken from ref 16. The black line corresponds to best fit of this data (R^2 = 0.992). The red points designate data for complexes **6**, **7**, **11**, **12** and $[Fe^{II}(tpy^{\bullet})_2]^0$ from ref 4 (the best fit line incorporating this data has a R^2 = 0.985).

function of charge (n = 0, 1−, 2−) are shown in Figure 5. Clearly, there is a linear correlation between the two, and filling the empty π^* LUMO of (bpy^0) in a stepwise fashion with two electrons leads to significant and detectable decreases in the $C_{py}-C_{py}$ and increases in the C−N bond distances. Similarly, the *average* $C_{py}-C_{py}$ distance in the series of chromium complexes $[Cr^{III}(^tbpy)_3]^m$ (m = 3+, 2+, 1+, 0) also varies in a linear fashion with charge (Figure 6).[2] Throughout this series (all m values from 3+ to 3− can be accessed) the central Cr ion retains a t_{2g}^3 electron configuration (i.e., it is always Cr^{III}).[2] It should be noted that calculation of average $C_{py}-C_{py}$ bond distances for $\{(bpy)_3\}^n$ using the values in Figure 5 yields close agreement with those in Figure 6, which indicates that these calculated values are characteristic of specific integer total charges. Therefore, in principle, the correlation in Figure 6 provides a means to identify the sum ligand charge $\{(bpy)_3\}^n$ (n = 0, 1−, 2−, 3−, 4−, 5−, 6−) in a given *tris*(bpy) complex solely from its high resolution X-ray crystal structure.

The structure of the complexes **1**, **2**, and **4** are shown in Figure 7, and selected bond distances are listed in Table 5. (Note, recently reported **3** exhibits a structure very similar to the aforementioned compounds.[11]) All of these neutral complexes crystallize isostructurally in the monoclinic space group $P2_1/c$ (No 14) with Z = 4. It is therefore quite remarkable that although none of these neutral molecules possess crystallographically imposed symmetry, in all three cases the C−C and C−N bond distances of the M(^{Me}bpy) chelates are identical within the 3σ limits.

The three effectively identical five-membered Mo(^{Me}bpy) chelate rings in complex **4** are slightly asymmetric, with one Mo−N bond distance being significantly longer than the other. The average difference between the two Mo−N bonds is 0.05 Å, where the estimated standard deviation (3σ) of the Mo−N bonds is 0.006 Å. This is in contrast to the reported structure of the chromium analogue $[Cr^{III}(^{Me}bpy^{\bullet})_3]^0$ (**3**), which crystallizes in the trigonal space group $R3c$ (No. 167) and contains three crystallographically equivalent Cr(^{Me}bpy) chelate rings, each of which possess two identical Cr−N bonds. Otherwise, the metrical details of the three (^{Me}bpy) ligands in **3** and **4** are

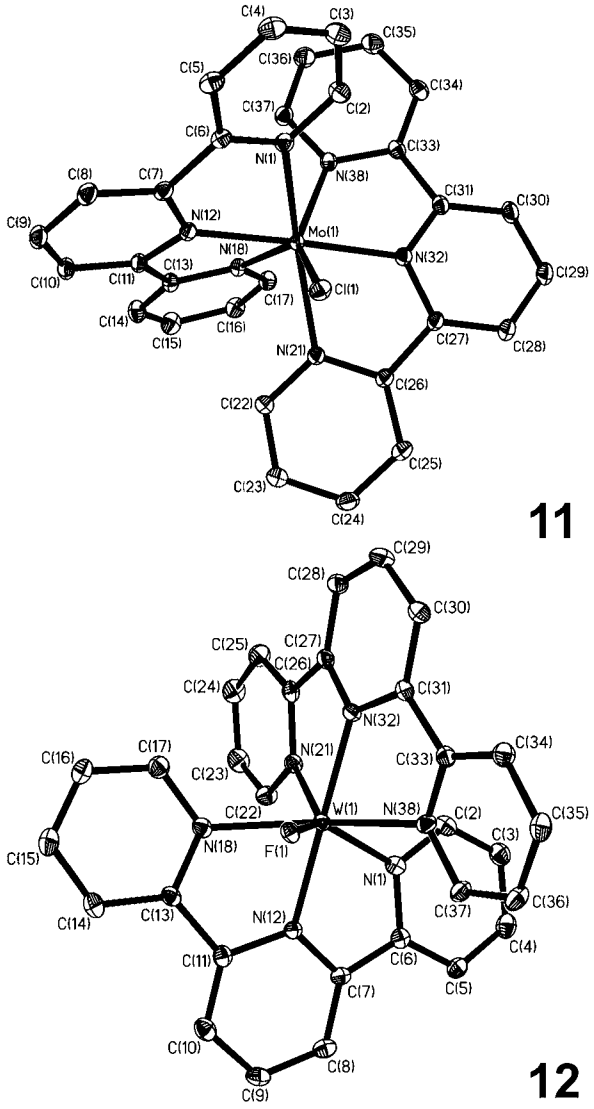

Figure 4. Structures of the monocationic components of **11** (top) and **12** (bottom) depicted using 40% probability ellipsoids. Hydrogen atoms have been omitted for clarity.

identical within error, and the average $C_{py}-C_{py}$ bond length in both is 1.426 Å, which is indicative of the presence of three $(^{Me}bpy^{\bullet})^-$ ligands (Figure 6). Thus, the electronic structure of **4** is analogous to that of **3** and is best described as $[Mo^{III}(^{Me}bpy^{\bullet})_3]^0$ (S = 0), with the three ligand-centered unpaired spins strongly antiferromagnetically coupled to those of the t_{2g}^3 Mo^{III} ion. Similarly, complex **1**, which is the first homoleptic bpy complex of titanium to be fully crystallographically characterized, displays an average $C_{py}-C_{py}$ bond length characteristic of $\{(bpy)_3\}^{3-}$, which equates to three $(bpy^{\bullet})^-$ ligands and leads to formulation as $[Ti^{III}(^{Me}bpy^{\bullet})_3]^0$ (S = 0). In this case, the singlet ground state presumably arises from antiferromagnetic coupling of the single metal-centered unpaired spin with that of a $(bpy^{\bullet})^-$, plus a further antiferromagnetic coupling of the two remaining ligand-centered spins. This ground state electronic structure is fully consistent with that recently proposed by us, based upon DFT calculations.[10]

Complex **2** is the first homoleptic bpy complex of vanadium to be characterized by X-ray crystallography. It contains six equivalent V−N bond with an average distance of 2.072 Å and

dx.doi.org/10.1021/ic402037e | Inorg. Chem. 2013, 52, 12763−12776

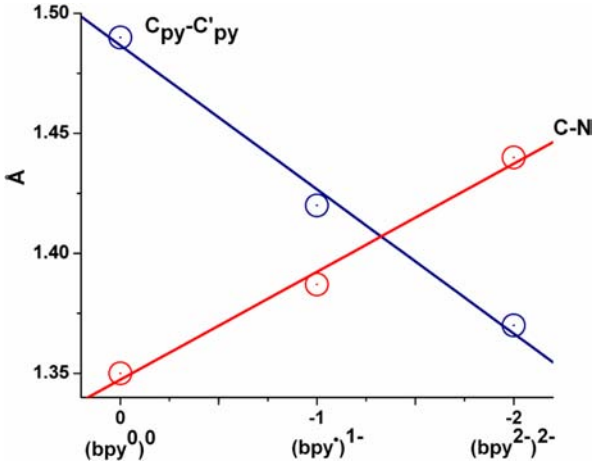

Figure 5. Linear correlation of the $C_{py}-C'_{py}$ (black circles) and average C−N (red circles) bond lengths (Å), taken from X-ray structures of uncoordinated bpy and alkali metal salts of the corresponding monoanion and dianion,[9] with the charge (n) of $(bpy)^n$. The best fit lines for both sets of data have $R^2 = 0.995$.

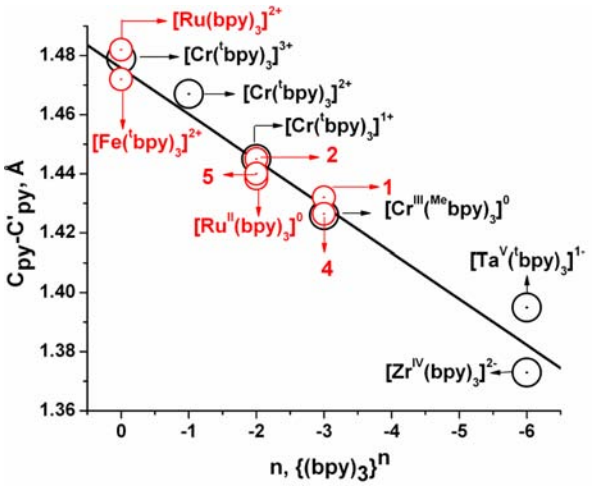

Figure 6. Average experimental $C_{py}-C_{py}$ bond distances (Å) as a function of total ligand $\{(bpy)_3\}^n$ charge (n). Data for $[Cr^{III}(^tbpy)_3]^{3+,\,2+,\,1+}$, $[Cr^{III}(^{Me}bpy)_3]^0$, $[Ta(^tbpy)_3]^-$ and $[Zr(bpy)_3]^{2-}$ (black points) taken from refs 2, 11, 10, and 24, respectively. The red points correspond to data for complexes **1**−**5**, taken from this work, and $[Ru^{II}(bpy)_3]^{2+/0}$ and $[Fe^{II}(^tbpy)_3]^{2+}$, taken from ref 4 and references therein. In all cases the experimental error is no larger than ±0.01 Å. The best fit of all data is given by the black line (R^2 = 0.982).

three equivalent ^{Me}bpy ligands displaying an average $C_{py}-C_{py}$ distance of 1.438 Å, which is indicative of the sum ligand charge $\{(bpy)_3\}^{2-}$ and corresponds to two π-radical anions, plus one neutral ligand. Thus, the central metal ion is V^{II}, it possesses the electronic structure $[V^{II}(bpy^\bullet)_2(bpy)]^0$, and the experimental observed $S = {}^1/_2$ ground state is obtained by antiferromagnetic coupling of the three metal-centered unpaired spins with those on the ligands. This picture is fully consistent with that previously established for $[V(^tbpy)_3]^0$ ($S = {}^1/_2$) using spectroscopy (EPR and V K-edge XAS) and DFT calculations.[3] Although it is clear why the structural parameters of the three ^{Me}bpy ligands **1**, **3**, and **4** are effectively identical in each case (they all contain three $(^{Me}bpy^\bullet)^-$ monoanions), that is not the case for complex **2**, which displays ligand mixed-valency. This is

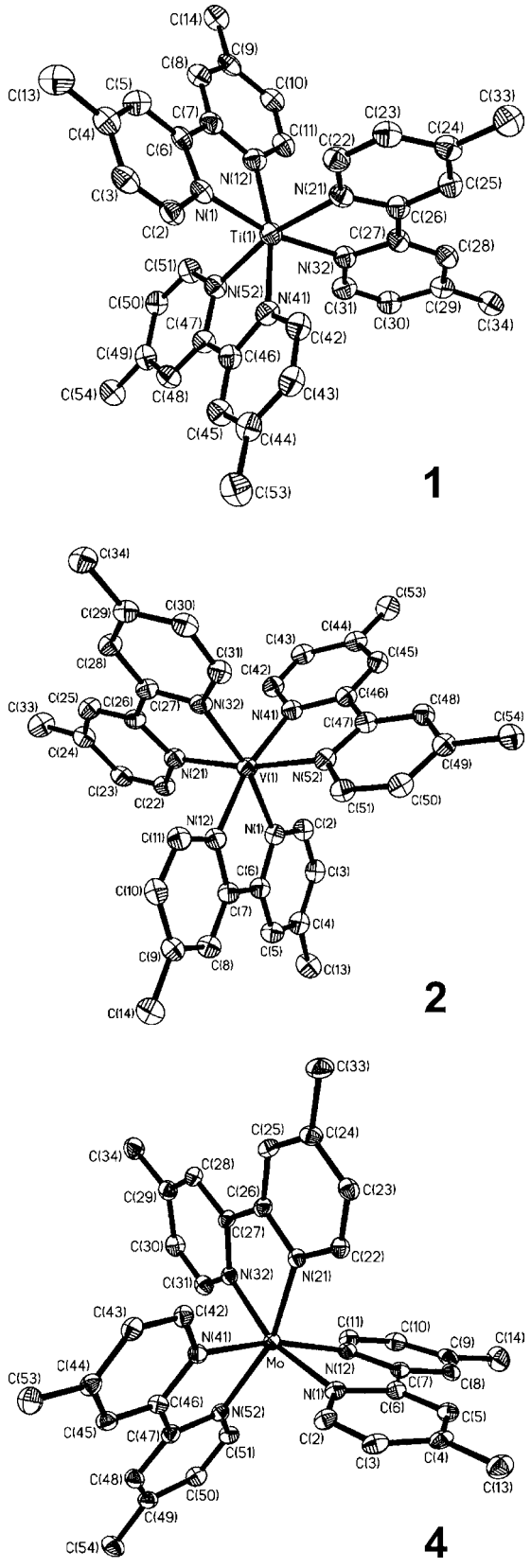

Figure 7. Structures of the neutral complexes **1** (top), **2** (middle), and **4** (bottom) depicted using 40% probability ellipsoids. Hydrogen atoms have been omitted for clarity.

presumably a consequence of charge delocalization and is in stark contrast to $[Cr^{III}(^tbpy^\bullet)_2(^tbpy)]^+$, wherein the differing

dx.doi.org/10.1021/ic402037e | Inorg. Chem. 2013, 52, 12763−12776

oxidation states of the ligands could be clearly discerned by X-ray crystallography.[2]

The diamagnetic complex **5**, shown in Figure 8, contains the seven-coordinate monocation $[MoF(^{Me}bpy)_3]^+$. The average

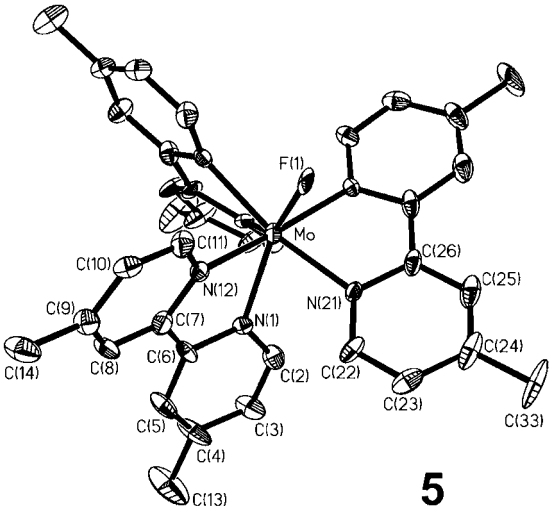

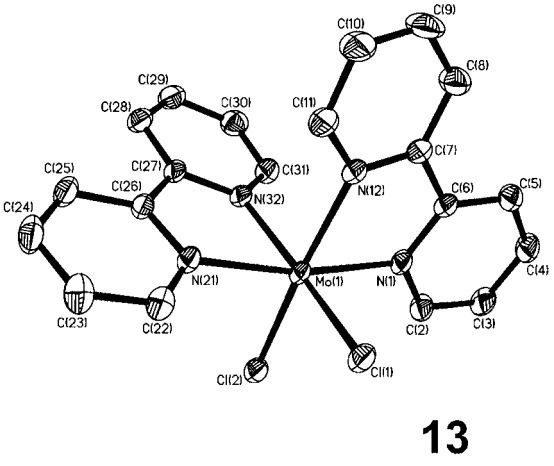

Figure 8. Structures of the monocationic components of **5** and **13** depicted using 40% probability ellipsoids. Hydrogen atoms have been omitted for clarity.

$C_{py}-C_{py}$ bond distance therein of 1.445 Å indicates that the sum ligand charge is $\{(^{Me}bpy)_3\}^{2-}$. Therefore, the electronic structure description $[Mo^{IV}F(^{Me}bpy^{\bullet})_2(^{Me}bpy^0)]^+$ appears to be appropriate, where the spins of a central $S = 1$ Mo^{IV} ion antiferromagnetically couple in an intramolecular fashion with two $(^{Me}bpy^{\bullet})^-$ π-radical anions to give the observed singlet ground state. Note that description of **5** as $[Mo^{III}F(^{Me}bpy^{\bullet})(bpy^0)_2]^+$ would result in a triplet ground state that would contradict the observed diamagnetism.

Lastly, complex **13** (Figure 8) consists of a monocation $[MoCl_2(bpy)_2]^+$ with an octahedral *cis*-MoN_4Cl_2 coordination environment, a chloride counteranion, and 2.5 molecules of methanol solvent. Its average $C_{py}-C_{py}$ bond length of 1.472 Å is consistent with the presence of two (bpy^0) ligands, from which we can infer the central Mo ion has a +III oxidation state and its electronic structure is $[Mo^{III}Cl_2(bpy^0)_2]^+$.

Electronic Spectra. The electronic spectra of the bpy complexes **1**, **2**, **4**, and **5**, and the tpy complexes **6**, **7**, and **9**, recorded in either THF or dichloromethane solution at ambient temperature in the range 300−1600 nm, are displayed in Figures 9 and 10, respectively, and this data summarized in

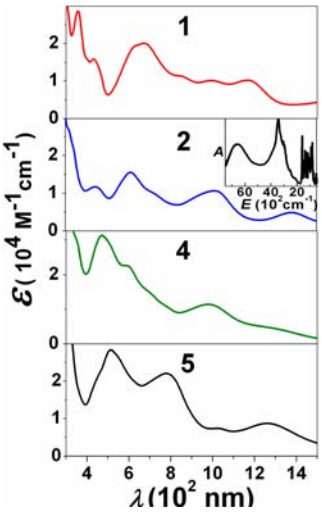

Figure 9. Electronic spectra recorded at 20 °C of **1** (red), **2** (blue), and **4** (green) in toluene solution, and **5** (black) in THF solution. The inset in the spectrum of **2** contains an IR spectrum of a KBr pellet of **2** (absorption in arbitrary units).

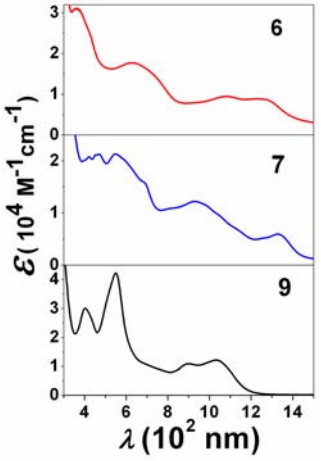

Figure 10. Electronic spectra recorded at 20 °C of **6** (red) and **7** (blue) in toluene solution, and **9** (black) in CH_2Cl_2 solution.

Table 7. The spectra of **3**,[11] **8**,[16] **9**,[16] **10**,[16] and **14**[17] have been reported previously, but those of **11** and **15**[18] have not and were not recorded in this study.

As reported by König and Kremer[25] in 1970, the electronic spectrum of the $(bpy^{\bullet})^-$ radical anion in dioxane solution exhibits three intense absorption bands at ~820, 520, and 385 nm, the former two of which display characteristic vibronic fine structure, with molar extinction coefficients ε of 0.4−1.5 × 10^4 M^{-1} cm^{-1}. The corresponding spectrum of the $(bpy^{2-})^{2-}$ dianion also exhibits two very intense bands at 610 and 370 nm. In both cases, these bands have been assigned to $\pi \rightarrow \pi^*$ and $\pi^* \rightarrow \pi^*$ transitions.

Unsurprisingly, the electronic spectrum of **1** (Figure 9) closely resembles that of $[Ti^{III}(bpy^{\bullet})_3]^0$ ($S = 0$), with both being dominated by intense bands in the visible and near-

dx.doi.org/10.1021/ic402037e | Inorg. Chem. 2013, 52, 12763−12776

Table 7. Electronic Spectra of Complexes 1−7 and 12−14, Recorded in THF Solution at 20°C

complex[a]	λ_{max}, nm (ε, M^{-1} cm^{-1})[b]
1	359 (2.8×10^4), 436 (1.6×10^4), 615 (sh), 678 (2.0×10^4), 850 (sh), 995 (1.0×10^4), 1170 (1.0×10^4)
2	310 (2.2×10^4), 445 (1.2×10^4), 612 (1.5×10^4), 710 (sh), 950 (sh), 1017 (1.1×10^4), 1380 (0.5×10^4), ~2800[c]
3	341 (2.7×10^4), 490 (sh), 521 (1.5×10^4), 580 (sh), 720 (sh), 1110 (0.6×10^4), 1300 (0.6×10^4)
4	350 (sh), 476 (3.1×10^4), 595 (2.3×10^4), 700 (sh), 983 (1.1×10^4), 1306 (1.5×10^4)
5	460 (sh), 513 (2.8×10^4), 781 (2.2×10^4), 1029 (0.8×10^4), 1265 (0.9×10^4)
6	363 (3.1×10^4), 633 (1.8×10^4), 700 (sh), 1079 (0.95×10^4), 1263 (0.9×10^4)
7	350 (sh), 423 (2.1×10^4), 466 (2.1×10^4), 547 (2.1×10^4), 600 (sh), 705 (sh), 929 (1.2×10^4), 1100 (sh), 1300 (0.6×10^4), 1410[c]
12	307 (4.8×10^4), 375 (sh), 509 (1.6×10^4), 620 (sh), 758 (1.2×10^4)
13	436 (2.1×10^3), 672 (sh, ~0.5×10^3)
14[d]	305 (2.7×10^4), 380 (sh, ~6×10^3), 438 (5.2×10^3), 550 (1.7×10^4), 745 (0.8×10^4), 940 (sh)

[a]Spectra of **8**, **9**, and **10** are detailed in ref 16, and that of **11** is not available. [b]The abbreviation sh refers to a shoulder. [c]Solid state spectrum (KBr disc). [d]Reference 17.

infrared regions associated with $\pi \rightarrow \pi^*$ and $\pi^* \rightarrow \pi^*$ transitions of the $(bpy^\bullet)^-$ radical anion (no d → d transitions were observed). This assignment is corroborated by the observation that its spectrum bears a strong similarity not only to that of $[Cr^{III}(bpy^\bullet)(^iPrNH_2)(CH_3CO_2)_2]^0$ (S = 1),[11] which contains a single $(bpy^\bullet)^-$ ligand, but also to those of **3**[11] (Table 7), $[Cr^{III}(^tbpy^\bullet)_3]^0$,[2] and $[Cr^{III}(bpy^\bullet)_3]^0$.[27,28] Similarly, the spectrum of the molybdenum complex **4** closely resembles those of the aforementioned $(bpy^\bullet)^-$-containing complexes.

Interestingly, in addition to four intense bands at 445, 612, 1017, and 1380 nm due to the presence of $(bpy^\bullet)^-$ radical anion(s), the spectrum of **2** possesses an additional transition in the near-infrared region at ~2800 nm. This band is assigned to a $(bpy^\bullet)^-$ → (bpy^0) ligand-to-ligand intervalence charge transfer (LLIVCT) transition, as was previously described by Heath et al.[29] for $[Ru^{II}(bpy^\bullet)(bpy^0)_2]^+$ and $[Ru^{II}(bpy^\bullet)_2(bpy^0)]^0$, and by us for $[V^{II}(^tbpy^\bullet)_2(^tbpy^0)]^0$.[3] This observation is fully consistent with the electronic structure description $[V^{II}(^{Me}bpy^\bullet)_2(^{Me}bpy^0)]^0$ forwarded above for **2**.

In stark contrast to those described previously, in the electronic spectrum of **13** (Table7) there is a marked absence of strong bands ($\varepsilon > 10^3$ M^{-1} cm^{-1}) above 700 nm. Instead, the lowest energy band at 672 nm is of moderate intensity ($\varepsilon = 0.5 \times 10^3$ M^{-1} cm^{-1}) and is most probably a d → d ($t_{2g}^3 \rightarrow t_{2g}^2e_g^1$) transition. This spectrum resembles that of $[Cr^{III}(bpy^0)_2(CH_3CO_2)_2]^+$,[11] and is consistent with the absence of both $(bpy^\bullet)^-$ and $(bpy^{2-})^{2-}$ anions.

Interestingly, intense bands (Table 7) have also been reported for the black complex $[Mo(bpy)_2(O^iPr)_2]^0$ (**14**),[17] which are characteristic of $(bpy^\bullet)^-$ ligands being present. However, the original authors stated that "the most distinguishing feature is that for 'normal' (neutral) bipy the intense $\pi \rightarrow \pi^*$ transition occurs at λ_{max} ~ 300 nm (ε ~ 15.000 M^{-1} cm^{-1}) where for $(bipy^\bullet)^-$ this transition moves to lower energy, λ_{max} ~ 380 nm[25]". In complex **14** the band at 380 nm is observed, but appears as a shoulder.[17] As a consequence, they proposed an electronic description with significant π-back-donation from a d^4 Mo^{II} center to the two neutral (bpy^0) ligands. However, we disagree with this interpretation and we take the electronic spectrum of **14** as a first indication that $(bpy^\bullet)^-$ radical anions are present.

The electronic spectra of the homoleptic tpy complexes of Ti (**6**), V (**7**), and Mo (**9**) are displayed in Figure 10 and summarized in Table 7, alongside the previously published data for the analogous Cr (**8**) and W (**10**) complexes.[16] The spectrum of $Li^+(tpy^\bullet)^-$ in diethylether solution has been reported to display intense bands at 370 nm (1.7×10^4), 380 (sh, 1.5×10^4), 440 (sh, 1.0×10^4), 600 (sh, 0.8×10^4), 620 (1.2×10^4), 710 (0.8×10^4), and 940 (0.3×10^4),[26] where the values in parentheses are molar extinction coefficients with units M^{-1} cm^{-1} and sh designates a shoulder. Unfortunately, that of the dianion $(tpy^{2-})^{2-}$ has yet to be published. The spectra of $[Fe^{II}(tpy^\bullet)_2]^0$ (S = 1), containing a high-spin Fe^{II} ion,[26] and $[Ru^{II}(tpy^\bullet)_2]^0$ (S = 0), containing a low-spin Ru^{II} ion,[30] have been reported and not only closely resemble one another but are dominated by $\pi \rightarrow \pi^*$ and $\pi \rightarrow \pi^*$ transitions that are very similar to those of the $(tpy^\bullet)^-$ radical anion. Indeed, observation of this spectral fingerprint in a given tpy complex can be taken as confirmation of the presence of $(tpy^\bullet)^-$ ligand(s) therein.

As shown in Figure 10, the spectra of **6**, **7**, and **9** are very similar to one another, with their most notable features being two intense bands ($\varepsilon > 10^4$ M^{-1} cm^{-1}) in the near-infrared (NIR) region between 900 and 1300 nm that are absent in $(tpy^\bullet)^-$-containing complexes. Instead, we tentatively assign these bands as $\pi^* \rightarrow \pi^*$ transitions of the coordinated $(tpy^{2-})^{2-}$ dianion, which is fully consistent with their X-ray structures, from which the presence of two dianions $(tpy^{2-})^{2-}$ and a tetravalent metal ion was inferred. Interestingly, the spectrum of **8**, $[Cr^{III}(tpy^\bullet)(tpy^{\bullet\bullet})]^0$, which contains both a $(tpy^\bullet)^-$ radical anion and a $(tpy^{\bullet\bullet})^{2-}$ dianion does not display these low energy features,[16] perhaps because the latter is present in its excited state.

DISCUSSION

Previously reported DFT calculations revealed that in the seven-membered electron transfer series $[Cr(bpy)_3]^m$ (m = 3+, 2+, 1+, 0, 1−, 2−, 3−) the Cr center retains a +III oxidation state throughout, which means that all redox processes are ligand-centered.[2] Furthermore, the average $C_{py}-C_{py}$ bond distance was found to decrease in a linear fashion with increasing total negative charge (n) of the three coordinated bpy ligands, $\{(bpy)_3\}^n$ (Figure 11). The agreement between experimentally determined (Figure 6) and calculated structures (Figure 11) was found to be excellent.[2] Furthermore, calculations of average $C_{py}-C_{py}$ distances for other $[M(bpy)_3]^m$ (M = Y, Ti, Zr, Hf and m = 0, 1−, 2−, 3−) redox series also fit into this correlation.[10]

It was demonstrated by McGrady and Goicoechea et al.[7,8] that the $C_{py}-C_{py}$ and average intrachelate C−N bond distances in the (bpy^0) and $(bpy^\bullet)^-$ ligands in their first-row transition metal $[M(bpy)(mes)_2]^{0,1-}$ (mes^- = 2,4,6−$Me_3C_6H_2$, M = Cr−Ni) complexes do *not* vary significantly with the d^n electron configuration of the metal ion. In other words, there is not a continuum of $C_{py}-C_{py}$ bond lengths and specific values correspond to specific bpy oxidation states. This implies, in agreement with our results,[10] that *N,N′*-coordinated neutral (bpy^0) and its monoanionic π-radical anion $(bpy^\bullet)^-$ are very weak π-acceptors and that any structural changes that result from such properties are not crystallographically detectable. In contrast, the *N,N′*-coordinated dianion $(bpy^{2-})^{2-}$ behaves as a

dx.doi.org/10.1021/ic402037e | Inorg. Chem. 2013, 52, 12763−12776

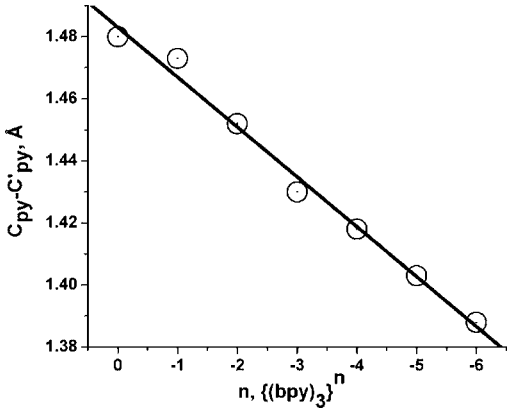

Figure 11. Plot of the average DFT calculated $C_{py}-C'_{py}$ bond length (Å) vs total charge (n) of $\{(bpy)_3\}^n$ in $[Cr^{III}(bpy)_3]^m$ (m = 3+, 2+, 1+, 0, 1−, 2−, 3−; $n = m - 3$), based upon data taken from ref 2 (the best fit line has a R^2 = 0.995).

π-donor ligand because of electron donation from the ligand HOMO into empty metal-centered t_{2g} orbitals (in O_h symmetry), and the $C_{py}-C_{py}$ distance varies somewhat with the d^n electron configuration.[10]

Table 8 summarizes the experimentally observed and calculated average $C_{py}-C_{py}$ bond distances of $[M(bpy)_3]^0$

Table 8. Summary of Experimental and Calculated Average $C_{py}-C'_{py}$ Distances (Å) in $[M(bpy)_3]^0$

	$C_{py}-C'_{py}$			
M	exp.	calcd.	$\{(bpy)_3\}^{n a}$	ref.
Ti	1.432	1.427	3−	10
Zr		1.425	4−	10
Hf		1.423	4−	10
V	1.438	1.438	2−	3
Cr	1.426	1.431	3−	2, 11
Mo	1.426		3−	this work
Fe		1.432	2−	4
Ru	1.440	1.435	2−	4, 12
Al		1.426	3−	4
Sc		1.429	3−	4

[a] n = 2− equates to a $(bpy^{\bullet})_2(bpy^0)$, n = 3− to a $(bpy^{\bullet})_3$, and n = 4− to a $(bpy^{\bullet})_2(bpy^{2-})$ electron configuration. In these cases, the physical oxidation state of the central metal ion is +II, +III, and +IV, respectively.

complexes, and Figures 6 and 11 illustrate the correlation between these values and the total charge (n) of the ligands $\{(bpy)_3\}^n$. Using these correlations, plus supplementary spectroscopic data, the electronic structures $[Ti^{III}(^{Me}bpy^{\bullet})_3]^0$ (S = 0; **1**),[31] $[V^{II}(^{Me}bpy^{\bullet})_2(^{Me}bpy^0)]^0$ ($S = {}^1/_2$; **2**), $[Cr^{III}(^{Me}bpy^{\bullet})_3]^0$ (S = 0; **3**),[11] and $[Mo^{III}(^{Me}bpy^{\bullet})_3]^0$ (S = 0; **4**) have been established. These assignments are in full agreement with those previously forwarded by us for the corresponding $[M(bpy)_3]^0$ complexes, based upon DFT and spectroscopy studies.[2,3,10,11] In all of these cases, plus the other $[M(bpy)_3]^0$ complexes we have studied, the central metal ions possesses a spectroscopic (physical) oxidation number ≥ +II, hence the label "low-valent" is misleading and should not be used to describe this class of compounds. Instead, it is more correct to consider them as Werner-type complexes displaying distorted MN_6 polyhedra (D_3) and either two or three *N,N′*-coordinated $(bpy^{\bullet})^-$ π-radical anions, with the balance made up by neutral (bpy^0) ligands.

Using the linear correlation of the average experimentally determined $C_{py}-C_{py}$ bond distances with the total charge (n) of $\{(tpy)_2\}^n$ (Figure 7) for the series $[Cr^{III}(tpy)_2]^m$ (m = 3+, 2+, 1+, 0),[16] the electronic structures of the octahedral complexes $[M(tpy)_2]^0$ (M = Ti, V, Cr, Mo, W) have been deduced based upon their crystallographically determined structures. When combined with minimal supplementary spectroscopic data, electronic structure of complexes **6** and **7** have been assigned as $[Ti^{IV}(tpy^{2-})_2]^0$ (S = 0) and $[V^{IV}(tpy^{2-})_2]^0$ ($S = {}^1/_2$), respectively. Conversely, this correlation indicates that the previously determined crystal structure of $[Fe(tpy)_2]^0$ is in full agreement with a description of it as $[Fe^{II}(tpy^{\bullet})_2]^0$ (S = 1), wherein a central high spin ferrous ion antiferromagnetically couples to two π-radical anions $(tpy^{\bullet})^-$, which was derived from a combination of magnetochemical measurements, Mössbauer spectroscopy, and DFT calculations.[4] Unfortunately, the crystal structure of $[Ru(tpy^{\bullet})_2]^0$ collected at 298 K is of fairly low quality, so unambiguous determination of n using the average $C_{py}-C_{py}$ distance (1.42 Å) is not possible in this case. However, an average $C_{py}-C_{py}$ distance of 1.450 Å has been calculated using DFT,[4] and according to the correlation in Figure 3 this corresponds to n = 2−, or two $(tpy^{\bullet})^-$ ligands. This leads to the electronic structure $[Ru^{II}(tpy^{\bullet})_2]^0$, which was calculated to contain a low-spin Ru^{II} ion and possess an S = 1 ground state because of ferromagnetic coupling of the ligand-centered unpaired spins.

Interestingly, pairs of $[M(^{Me}bpy)_3]^m$ and $[M(tpy)_2]^m$ complexes containing common metals can exhibit different physical oxidation states. For example, in the case of titanium, complex **1** possesses three $(^{Me}bpy^{\bullet})^-$ ligands but **6** contains two diamagnetic $(tpy^{2-})^{2-}$ dianions. In other words, whereas the physical oxidation state of Ti is +III (d^1) in **1**, it is +IV (d^0) in **6**. Additionally, the pair of complexes **2** and **7** contain V^{II} and V^{IV} ions, respectively; and the Mo ion in complexes **4** and **9**[16] possess respective oxidation states of +III and +IV. In contrast, the corresponding pair of chromium complexes, **3**[2] and **8**,[16] both contain Cr^{III} centers. The differing physical oxidation states in bpy and tpy complexes containing the same metal ion highlights the fact that these ligands are not simply interchangeable. This probably stems from the interplay of several factors, including: the differing symmetries of the MN_6 polyhedra (D_3 in $[M(bpy)_3]^m$ and D_{2d} in $[M(tpy)_2]^m$), which would be expected to manifest as different spin exchange coupling pathways (J-values); the greater ligand field exerted by three (bpy^0) ligands relative to two (tpy^0) ligands, which is clearly demonstrated by the observation that $[Fe^{II}(^tbpy^{\bullet})_2(^tbpy^0)]^0$ contains low-spin Fe^{II} and $[Fe^{II}(tpy^{\bullet})_2]^0$ contains high-spin Fe^{II};[4] and the differing energies of the LUMOs of the (tpy^0) and (bpy^0) ligands (more extensive delocalization in the former might be expected to equate to a more energetically accessible LUMO and easier reduction).

Using the aforementioned correlations (Figures 3 and 6) it has also been possible to determine the total ligand charge, $\{bpy)_3\}^n$ and $\{(tpy)_2\}^n$, for the seven-coordinate monocations in **5** and **11** (n = 2−). On this basis, the electronic structures of these species are best formulated as $[Mo^{IV}F(^{Me}bpy^{\bullet})_2(^{Me}bpy^0)](PF_6)$ (**5**) and $[Mo^{IV}Cl(tpy^{\bullet})_2](PF_6)$ (**11**). It was established by magnetochemical measurements that complexes **5** and **11** both possess a singlet ground state, which in both cases is attained via intramolecular antiferro-

dx.doi.org/10.1021/ic402037e | Inorg. Chem. 2013, 52, 12763−12776

Table 9. Comparison of Bond Distances (Å) in the *N,N′*-Coordinated bpy Ligands in 14 and 15 with Those in Uncoordinated (bpy^0) and an Alkali Metal Salt of $(bpy^{\bullet})^{-}$[a]

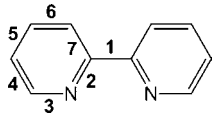

compound	bond, (Å) 1	2	3	4	5	6	7	ref.
(bpy^0)	1.490(3)	1.346(2)	1.341(2)	1.384(2)	1.383(3)	1.385(2)	1.394(2)	9a
K($bpy^{\bullet}$)(en)	1.431(3)	1.390(3)	1.337(3)	1.373(3)	1.404(3)	1.365(3)	1.428(3)	9b
14 (1st $bpy^{\bullet}$)	1.424(4)	1.370(4)	1.373(4)	1.357(4)	1.417(5)	1.371(5)	1.412(4)	9a
14 (2nd $bpy^{\bullet}$)	1.425(4)	1.385(4)	1.376(4)	1.358(4)	1.416(5)	1.363(4)	1.410(4)	
15 (1st $bpy^{\bullet}$)	1.412(4)	1.383(3)	1.374(6)	1.361(5)	1.413(5)	1.358(5)	1.414(4)	18
15 (2nd $bpy^{\bullet}$)	1.409(4)	1.380(3)	1.374(3)	1.365(4)	1.404(5)	1.360(5)	1.407(4)	

[a]A bond labeling scheme is provided above.

magnetic coupling between two π-radical anions ($(bpy^{\bullet})^{-}$ or $(tpy^{\bullet})^{-}$) and a central high-spin Mo^{IV} ion. In contrast, the resolution of the X-ray structure of the heptacoordinate complex **12** is insufficient for a definitive electronic structure assignment, and although the average tpy structural parameters imply a $[W^{V}F(tpy^{\bullet})(tpy^{2-})](PF_6)$ formulation, in which its diamagnetic ground state derives from antiferromagnetic coupling of a single $(tpy^{\bullet})^{-}$ radical anion with the central W^{V} ion, $[W^{VI}F(tpy^{2-})_2]^{+}$ and $[W^{IV}F(tpy^{\bullet})_2]^{+}$ are also possible. This serves to highlight the importance of very high resolution X-ray crystallography in complexes containing potentially non-innocent ligands, and the dangers of attempting to assign ligand oxidation states from crystal structure parameters in its absence.

It is now of interest to use our correlations to examine the electronic structures of other compounds, such as $[Mo(O^{i}Pr)_2(bpy)_2]^0$ (S = 0; **14**)[9a,17] and its tungsten analogue $[W(OAr)_2(bpy)_2]^0$ (S = 0; **15**), where OAr = 2,3,5,6-tetraphenylphenolate.[18] Complex **14** possesses interesting magnetochemical behavior, with an effective magnetic moment that increases from 1.3 to 1.93 μ_B in the temperature range 100−300 K, which was successfully modeled using the Bleany−Bowers equation for two antiferromagnetically coupled electrons with a coupling constant of −79 cm^{-1} ($\hat{H} = -2J \cdot S_1 \cdot S_2$; $S_1 = S_2 = {}^1/_2$).[17] The original authors *incorrectly* explained this behavior using a model involving a spin-crossover equilibrium between the high-spin (S = 1) and low-spin (S = 0) states of a Mo^{II} center, thereby rendering the two *N,N′*-coordinated bpy ligands neutral. Two other models were also discussed, (1) $[Mo^{IV}(O^{i}Pr)_2(bpy^{\bullet})_2]^0$ and (2) $[Mo^{III}(O^{i}Pr)_2(bpy^0)(bpy^{\bullet})]^0$, but were rejected. This is perhaps somewhat understandable because although an excellent crystal structure of uncoordinated $(bpy)^0$ was available at that time,[9a] that was not the case for an alkali metal salt of the π-radical anion. Such a structure, namely K($bpy^{\bullet}$)(en) (en = ethylenediamine),[9b] is now available, and the pertinent structural parameters of this species and uncoordinated $(bpy)^0$ are listed in Table 9, alongside those of complexes **14** and **15**.

Interestingly, the average $C_{py}-C'_{py}$ bond lengths in both complexes **14** and **15**[18] are very similar at 1.425 and 1.411 Å, respectively, and agree very well with the presence of two $(bpy^{\bullet})^{-}$ ligands. In contrast, the structural parameters of the *N,N′*-coordinated bpy ligands in the isostructural complexes $[Zn^{II}(OAr')_2(bpy^0)_2]^0$ and $[Cd^{II}(OAr')_2(bpy^0)_2]^0$, where $(OAr')^{-}$ corresponds to 2-chloro-4-nitrophenolate, (average $C_{py}-C'_{py}$ distances of 1.493 and 1.483 Å, respectively)[32] are clearly those of *neutral* (bpy^0). Thus, the electronic structures of both **14** and **15** are best described as $[M^{IV}(bpy^{\bullet})_2(OR)_2]^0$ (M = Mo, W). Given that the magnitude of the exchange coupling constant J for **14** of −79 cm^{-1} is relatively small and comparable to those reported for $[Al^{III}(bpy^{\bullet})_3]^0$ and $[Sc^{III}(bpy^{\bullet})_3]^0$ (J = −79 and −139 cm^{-1}, respectively),[33] the S = 0 ground state of this complex most probably results from intramolecular antiferromagnetic coupling of the bpy-centered unpaired spins. In this scenario, the d^2 Mo^{IV} ion in **14**, and presumably also the W^{IV} ion in **15**, would be low-spin (S = 0).

For comparison, the average $C_{py}-C_{py}$ distance in the monocationic component of **13**, which contains a central d^3 Mo^{III} ion, is 1.472 Å and in $[Mo^0(bpy)_2(CO)_2]^0$, which contains a Mo^0 center (d^6), it is 1.465 Å.[34] These bond lengths are, in both cases, very similar to those of uncoordinated (bpy^0). A similar conclusion is reached for $[Mo(bpy^0)(CO)_4]^0$, where a $C_{py}-C_{py}$ distance of 1.483 Å is observed.[35] Hence, even when bound to an electron rich transition metal ion an *N,N′*-coordinated (bpy^0) does not show significant structural changes, which once again highlights the fact that this ligand is a very poor π-acceptor.[6,7]

With this in mind, it is noteworthy that in $[Ti(bpy)_2(OAr'')_2]^0$ ($(OAr'')^{-}$ = 2,6-*bis*(1-methylethyl)phenolate) the average $C_{py}-C'_{py}$ bond length at 1.428 Å,[19] which is in excellent agreement with the corresponding distance in the alkali metal salt K($bpy^{\bullet}$)(en).[9b] On this basis, we suggest that its electronic structure should be described as $[Ti^{IV}(bpy^{\bullet})_2(OAr)_2]^0$, with the experimentally oberved S = 0 ground state originating from intramolecular antiferromagnetic coupling of the ligand-centered unpaired spins, and not the $[Ti^{II}(bpy^0)_2(OAr)_2]^0$ formulation forwarded by the original authors.

CONCLUSION

In this study it is shown that the total ligand charges (n) in transition metal complexes containing $\{(bpy)_3\}^n$ (n = 0 to 6−) and $\{(tpy)_2\}^n$ (n = 0 to 4−) can be determined experimentally by high resolution X-ray crystallography at cryogenic temperatures in cases where the C−C and C−N bond distances possess estimated standard deviations $\sigma \leq 0.004$ Å. This is because the average $C_{py}-C_{py}$ bond distances in both bpy and tpy vary in a linear fashion with charge and exhibit a particular range of values for a specific n. Hence, the oxidation state of the transition metal ion in neutral $[M(bpy)_3]^0$ and $[M(tpy)_2]^0$

dx.doi.org/10.1021/ic402037e | Inorg. Chem. 2013, 52, 12763−12776

complexes can then be defined as $-n$ and $-m$. In the present series of compounds, **1**−**4** and **6**−**10**, no case has been identified in which the oxidation state of the central metal ion is smaller than +II. Therefore, describing these compounds as "low-valent" is clearly incorrect, and using the term "highly reduced" would be much more appropriate.

■ ASSOCIATED CONTENT

Supporting Information

Crystallographic information files (cif) and magnetic susceptibility data. This material is available free of charge via the Internet at http://pubs.acs.org.

■ AUTHOR INFORMATION

Corresponding Author

*E-mail: karl.wieghardt@cec.mpg.de.

Notes

The authors declare no competing financial interest.

■ ACKNOWLEDGMENTS

M.W. thanks the Max Planck Society for financial support and Ms. Heike Schucht and Mr. Andreas Göbels for technical assistance.

■ REFERENCES

(1) An excellent review of the early coordination chemistry of 2,2′-bipyridine is available: Constable, , E. C. . In *Advances in Inorganic Chemistry*; Sykes, , A. G., Ed.; Academic Press: San Diego, CA, **1989**,; Vol. *34*,, p 1. Similarly, for 2,2′-terpyridine by the same author in *Advances in Inorganic Chemistry*; Sykes, , A. G., Ed.; Academic Press: San Diego, CA, **1986**,; Vol. *31*,, p 69.

(2) Scarborough, C. C.; Sproules, S.; Weyhermüller, T.; DeBeer, S.; Wieghardt, K. *Inorg. Chem.* **2011**, *50*, 12446.

(3) Bowman, A. C.; Sproules, S.; Wieghardt, K. *Inorg. Chem.* **2012**, *51*, 3707.

(4) England, J.; Scarborough, C. C.; Weyhermüller, T.; Sproules, S.; Wieghardt, K. *Eur. J. Inorg. Chem.* **2012**, 4605.

(5) Scarborough, C. C.; Sproules, S.; Doonan, C. J.; Hagen, K. S.; Weyhermüller, T.; Wieghardt, K. *Inorg. Chem.* **2012**, *51*, 6969.

(6) Scarborough, C. C.; Wieghardt, K. *Inorg. Chem.* **2011**, *50*, 9773.

(7) Irwin, M.; Doyle, L. R.; Krämer, T.; Herchel, R.; McGrady, J. E.; Goicoechea, J. M. *Inorg. Chem.* **2012**, *51*, 12301.

(8) Irwin, M.; Jenkins, R. K.; Denning, M. S.; Krämer, T.; Grandjean, F.; Long, G. J.; Herchel, R.; McGrady, J. E.; Goicoechea, J. M. *Inorg. Chem.* **2010**, *49*, 6160.

(9) (a) Chisholm, M. M.; Huffman, J. C.; Rothwell, I. P.; Bradley, P. G.; Kress, N.; Woodruff, J. M. *J. Am. Chem. Soc.* **1981**, *103*, 4945. (b) Gore-Randall, E.; Irwin, M.; Denning, M. S.; Goicoechea, J. M. *Inorg. Chem.* **2009**, *48*, 8304. (c) Echegoyen, L.; DeCiam, A.; Fischer, J.; Lehn, J.-M. *Angew. Chem., Int. Ed.* **1991**, *30*, 838. (d) Bock, H.; Lehn, J.-M.; Pauls, J.; Holl, S.; Krenzel, V. *Angew. Chem., Int. Ed.* **1999**, *38*, 952.

(10) Bowman, A. C.; England, J.; Sproules, S.; Weyhermüller, T.; Wieghardt, K. *Inorg. Chem.* **2013**, *52*, 2242.

(11) Wang, M.; England, J.; Weyhermüller, T.; Kokatam, S.-L.; Pollock, C. J.; DeBeer, S.; Shen, J.; Yap, G. P. A.; Theopold, K. H.; Wieghardt, K. *Inorg. Chem.* **2013**, *52*, 4472.

(12) Pérez-Cardero, E. E.; Campana, C.; Echegoyen, L. *Angew. Chem., Int. Ed. Engl.* **1997**, *36*, 137.

(13) (a) Al: Herzog, S.; Geisler, K.; Präkel, H. *Angew. Chem.* **1963**, *75*, 94. (b) Mg: Herzog, S.; Grimm, V. *Z. Chem.* **1968**, *8*, 186. (c) Sc: Wulf, E.; Herzog, S. *Z. Anorg. Allg. Chem.* **1972**, *387*, 81. (d) Y: Herzog, S.; Gustav, K. *Z. Naturforsch.* **1962**, *17b*, 62. (e) Ti: Herzog, S.; Taube, R. *Z. Anorg. Allg. Chem.* **1960**, *306*, 177. (f) Zr: Herzog, S.; Zühlke, H. *Z. Naturforsch.* **1960**, *15b*, 466. (g) Hf: Quirk, J.; Wilkinson, G. *Polyhedron* **1982**, *1*, 209. (h) V: Herzog, S. *Chem. Technol.* **1954**, *6*, 338. (i) Nb: Herzog, S.; Schuster, R. *Z. Naturforsch.* **1962**, *17b*, 62. (j) Ta: ref 13g. (k) Cr: Herzog, S.; Renner, K.-C.; Schön, W. *Z. Naturforsch.* **1957**, *12b*, 809. (l) Mo: Herzog, S.; Schneider, I. *Z. Chem.* **1962**, *2*, 24. (m) Mn: Herzog, S.; Schmidt, M. *Z. Chem.* **1962**, *2*, 24. (n) Re: ref 13g. (o) Fe: Herzog, S.; Präkel, H. *Z. Chem.* **1965**, *5*, 469. (p) Hall, F. S.; Reynolds, W. L. *Inorg. Chem.* **1966**, *5*, 931. (q) Ru: Pérez-Cordero, E.; Buigas, R.; Brady, N.; Echegoyen, L.; Arana, C.; Lehn, J.-M. *Helv. Chim. Acta* **1994**, *77*, 1222. (r) Os: ref 13p. (s) Co: Herzog, S.; Klausch, R.; Lantos, J. *Z. Chem.* **1964**, *4*, 150. (t) Albrecht, G. *Z. Chem.* **1963**, *3*, 182.

(14) (a) Ti: Behrens, H.; Brandl, H. *Z. Naturforsch.* **1967**, *22b*, 1216. (b) V: Herzog, S.; Aul, H. *Z. Chem.* **1966**, *6*, 382. (c) Behrens, H.; Brandl, H.; Lutz, K. *Z. Naturforsch.* **1967**, *22b*, 99. (d) Cr: ref 14b. and 14g; (e) Mo: Behrens, H.; Anders, U. *Z. Naturforsch.* **1964**, *19b*, 767. (f) DuBois, D. W.; Iwamoto, R. T.; Kleinberg, J. *Inorg. Chem.* **1970**, *9*, 968. (g) W: Behrens, H.; Meyer, K.; Müller, A. *Z. Naturforsch.* **1965**, *20b*, 74. (h) Ru: Pyo, S.; Pérez-Cordero, E.; Bott, S. G.; Echegoyen, L. *Inorg. Chem.* **1999**, *38*, 3337. (i) Os: ref 13p.

(15) ^{Me}bpy = 4,4′-dimethyl-2,2′-bipyridine; ^{t}bpy = 4,4′-di-*tert*-butyl-2,2′-bipyridine.

(16) Scarborough, C. C.; Lancaster, K. M.; DeBeer, S.; Weyhermüller, T.; Sproules, S.; Wieghardt, K. *Inorg. Chem.* **2012**, *51*, 3718.

(17) Chisholm, M. H.; Kober, E. M.; Ironmonger, D. J.; Thornton, P. *Polyhedron* **1985**, *4*, 1869.

(18) Lentz, M. R.; Fanwick, P. E.; Rothwell, I. P. *Organometallics* **2003**, *22*, 2259.

(19) Durfee, L. D.; Fanwick, P. E.; Rothwell, I. P. *J. Am. Chem. Soc.* **1987**, *109*, 4720.

(20) Stoffelbach, F.; Saurenz, D.; Poli, R. *Eur. J. Inorg. Chem.* **2001**, 2699.

(21) *SADABS, Bruker-Siemens Area Detector Absorption and Other Corrections*, Version 2008/1; Sheldrick, G. M. Universität Göttingen: Göttingen, Germany, 2006.

(22) *ShelXTL 6.14*; Bruker AXS Inc.: Madison, WI, 2003.

(23) *ShelXL97*; Sheldrick, G. M. Universität Göttingen: Göttingen, Germany, 1997.

(24) Rosa, P.; Mèzailless, N.; Ricard, L.; Mathey, F.; LeFloch, P. *Angew. Chem., Int. Ed.* **2000**, *39*, 1823.

(25) König, E.; Kremer, S. *Chem. Phys. Let.* **1970**, *5*, 87.

(26) Braterman, P. S.; Song, J.-I.; Peacock, R. D. *Inorg. Chem.* **1992**, *31*, 555.

(27) (a) König, E.; Herzog, S. *J. Inorg. Nucl. Chem.* **1970**, *32*, 613. (b) Kaizu, Y.; Yazaki, T.; Torii, Y.; Kobayashi, H. *Bull. Chem. Soc. Jpn.* **1970**, *43*, 2068. (c) Pappalardo, R. *Inorg. Chim. Acta* **1968**, *2*, 209.

(28) König, E.; Herzog, S. *J. Inorg. Nucl. Chem.* **1970**, *32*, 585.

(29) Heath, G. A.; Yellowlees, L. J.; Braterman, P. S. *Chem. Phys. Lett.* **1982**, *92*, 646.

(30) Berger, R. M.; McMillin, D. R. *Inorg. Chem.* **1988**, *27*, 4245.

(31) The $[Ti^{III}(bpy^{\bullet})_3]^0$ formulation was previously proposed based upon 200 MHz ^{1}H NMR spectroscopy measurements: Flamini, A.; Giuliani, A. M. *Inorg. Chim. Acta* **1986**, *112*, L7−L9.

(32) (a) Evans, C. C.; Masse, R.; Nicoud, J.-F.; Bagieu-Beucher, M. *J. Mater. Chem.* **2000**, *10*, 1419. (b) Evans, C. C.; Le Fur, Y.; Masse, R. *Z. Kristallogr. − New Cryst. Struct.* **2001**, *216*, 61.

(33) (a) Inoue, M.; Horiba, T.; Hara, K. *Bull. Chem. Soc. Jpn.* **1978**, *51*, 3073. (b) Wulf, E.; Herzog, S. *Z. Anorg. Allg. Chem.* **1972**, *387*, 81.

(34) Chisholm, M. H.; Conner, J. A.; Huffman, J. C.; Kober, E. M.; Overton, C. *Inorg. Chem.* **1984**, *23*, 2298.

(35) Braga, S. S.; Coelho, A. C.; Goncalves, I. S.; Paz, F. A. A. *Acta Crystallogr., Sect. E: Struct. Rep.* **2007**, *63*, m780.